sion in embryonic development and immune responses rather than stress-induced apoptosis.

Acknowledgments—We thank Dr. Izumu Saito and RIKEN BRC for providing us with adenovirus-encoding Cre recombinase. We also thank Dr. James R. Woodgett for suggestions and criticism.

REFERENCES

1. Peng, L., Deepak, N., Imawati, B., Srinivasa. M. S., Manzoor A., Emad, S. A., and Xiaodong, W. (1997) *Cell* **91**, 479–489
2. Orrenius, S., Zhivotovsky, B., and Nicotera, P. (2003) *Nature Rev. Mol. Cell Biol.* **4**, 552–565
3. Yoshida, H., Kong, Y.-Y., Yoshida, R., Elia, A. J., Hakem, A., Hakem, R., Penninger, J. M., and Mak, T. W. (1998) *Cell* **94**, 739–750
4. Davis, R. J. (2000) *Cell* **103**, 239–252
5. Chang, L., and Karin M. (2001) *Nature* **410**, 37–40
6. Manning, A. M., and Davis, R. J. (2003) *Nature Rev. Mol. Drug Disc.* **2**, 554–565
7. Lawler, S., Fleming, Y., Goedert, M., and Cohen, P. (1998) *Curr. Biol.* **8**, 1387–1390
8. Wada, T., Nakagawa, K., Watanabe, T., Nishitai, G., Seo, J., Kishimoto, H., Kitagawa, D., Sasaki, T., Penninger, J. M., Nishina, H., and Katada, T. (2001) *J. Biol. Chem.* **276**, 30892–30897
9. Kishimoto, H., Nakagawa, K., Watanabe, T., Kitagawa, D., Momose, H., Seo, J., Nishitai, G., Shimizu, N., Ohata, S., Tanemura, S., Asaka, S., Goto, T., Fukushi, H., Yoshida, H., Suzuki, A., Sasaki, T., Wada, T., Penninger, J. M., Nishina, H., and Katada, T. (2003) *J. Biol. Chem.* **278**, 16595–16601
10. Ganiatsas, S., Kwee, L., Fujiwara, Y., Perkins, A., Ikeda, T., Labow, M. A., and Zon, L. I. (1998) *Proc. Natl. Acad. Sci. U. S. A.* **95**, 6881–6886
11. Nishina, H., Vaz, C., Billia, P., Nghiem, M., Sasaki, T., Pompa, J. L., Furlonger, K., Paige, C., Hui, C.-C., Fischer, K. D., Kishimoto, H., Iwatsubo, T., Katada, T., Woodgett, J. R., and Penninger, J. M. (1999) *Development* **126**, 505–516
12. Watanabe, T., Nakagawa, K., Ohata, S., Kitagawa, D., Nishitai, G., Seo, J., Tanemura, S., Shimizu, N., Kishimoto, H., Wada, T., Aoki, J., Arai, H., Iwatsubo, T., Mochita, M., Watanabe, T., Satake, M., Ito, Y., Matsuyama, T., Mak, T. W., Penninger, J. M., Nishina, H., and Katada, T. (2002) *Dev. Biol.* **250**, 332–347
13. Lin, A. (2002) *BioEssays* **25**, 17–24
14. Kuan, C.-Y., Yang, D. D., Roy, D. R. S., Davis, R. J., Rakic, P., and Flavell, R. A. (1999) *Neuron* **22**, 667–676
15. Sabapathy, K., Jochum, W., Hochedlinger, K., Chang, L., Karin, M., and Wagner, E. F. (1999) *Mech. Dev.* **89**, 115–124
16. Tournier, C., Hess, P., Yang, D. D., Xu, J., Turner, T. K., Nimnual, A., Bar-Sagi, D., Jones, S. N., Flavell, R. A., and Davis, R. J. (2000) *Science* **288**, 870–874
17. Tournier, C., Dong, C., Turner, T. K., Jones, S. N., Flavell, R. A., and Davis, R. J. (2001) *Genes Dev.* **15**, 1419–1426
18. Aoki, H., Kang, P. M., Hampe, J., Yoshimura, K., Noma, T., Matsuzaki, M., and Izumo, S. (2002) *J. Biol. Chem.* **277**, 10244–10250
19. Chauhan, D., Li, G., Hideshima, T., Podar, K., Mitsiades, C., Mitsiades, N., Munshi, N., Kharbanda, S., and Anderson, K. C. (2003) *J. Biol. Chem.* **278**, 17593–17596
20. Nishina, H., Fischer, K. D., Radvanyi, L., Shahinian, A., Hakem, R., Rubie, E. A., Bernstein, A., Mak, T. W., Woodgett, J. R., and Penninger, J. M. (1997) *Nature* **385**, 350–353
21. Kanegae, Y., Lee, G., Sato, Y., Tanaka, M., Nakai, M., Sasaki, T., Sugano, S., and Saito, I. (1995) *Nucleic Acids Res.* **23**, 3816–3821
22. Kitagawa, D., Tanemura, S., Ohata, S., Shimizu, N., Seo, J., Nishitai, G., Watanabe, T., Nakagawa, K., Kishimoto, H., Wada, T., Tezuka, T., Yamamoto, T., Nishina, H., and Katada, T. (2002) *J. Biol. Chem.* **277**, 366–371
23. Nishina, H., Bachmann, M., Oliveira-dos-Santos, A. J., Kozieradzki, I., Fischer, K. D., Odermatt, B., Wakeham, A., Shahinian, A., Takimoto, H., Bernstein, A., Mak, T. W., Woodgett, J. R., Ohashi, P. S., and Penninger, J. M. (1997) *J. Exp. Med.* **186**, 941–953
24. Beere, H. M., Wolf, B. B., Cain, K., Mosser, D. D., Mahboubi, A., Kuwana, T., Tailor, P., Morimoto, R. I., Cohen, G. M., and Green, D. R. (2000) *Nat. Cell Biol.* **2**, 469–475
25. Saleh, A., Srinivasula, S. M., Balkir, L., Robbins, P. D., and Alnemri, E. S. (2000) *Nat. Cell Biol.* **2**, 476–483
26. Bruey, J.-M., Ducasse, C., Bonniaud, P., Ravagnant, L., Susin, S. A., Diaz-Latoud, C., Gurbuxani, S., Arrigo, A.-P., Kroemer, G., Solary, E., and Garrido, C. (2000) *Nat. Cell Biol.* **2**, 645–652
27. Xia, Z. G., Dickens, M., Raigeaud, J., Davis, R. J., and Greenberg, M. E. (1995) *Science* **270**, 1326–1331
28. Putcha, G. V., Le, S., Frank, S., Besirli, C. G., Clark, K., Chu, B., Alix, S., Youle, R. J., LaMarche, A., Maroney, A. C., and Johnson, E. M., Jr. (2003) *Neuron* **38**, 899–914
29. Su, B., Jacinto, E., Hibi, M., Kallunki, T., Karin, M., and Benneriah, Y. (1994) *Cell* **77**, 727–736
30. Conze, D., Krahl, T., Kennedy, N., Weiss, L., Lumsden, J., Hess, P., Flavell, R. A., Gros, G. L., Davis, R. J., and Rincon M. (2002) *J. Exp. Med.* **195**, 811–823
31. Krause, A., Holtmann, H., Eickemeier, S., Winzen, R., Szamel, M., Resch, K., Saklatvala, J., and Kracht, M. (1998) *J. Biol. Chem.* **273**, 23681–23689
32. Holtmann, H., Enninga, J., Kalble, S., Thiefes, A., Dorrie, A., Broemer, M., Winzen, R., Wilhelm, A., Ninomiya-Tsuji, J., Matsumoto, K., Resch, K., and Kracht, M. (2001) *J. Biol. Chem.* **276**, 3508–3516

ELSEVIER

Mechanisms of Development 121 (2004) 791–802

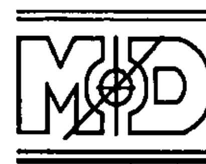

www.elsevier.com/locate/modo

Research paper

Mutations affecting liver development and function in Medaka, *Oryzias latipes*, screened by multiple criteria

Tomomi Watanabe[a], Satoshi Asaka[a], Daiju Kitagawa[a], Kota Saito[a], Ryumei Kurashige[a], Takao Sasado[b], Chikako Morinaga[b], Hiroshi Suwa[b], Katsutoshi Niwa[b], Thorsten Henrich[b], Yukihiro Hirose[c], Akihito Yasuoka[d], Hiroki Yoda[e], Tomonori Deguchi[e], Norimasa Iwanami[f], Sanae Kunimatsu[f], Masakazu Osakada[e], Felix Loosli[h], Rebecca Quiring[h], Matthias Carl[h], Clemens Grabher[h], Sylke Winkler[h], Filippo Del Bene[h], Joachim Wittbrodt[h], Keiko Abe[d], Yousuke Takahama[f], Katsuhito Takahashi[g], Toshiaki Katada[a], Hiroshi Nishina[a,*], Hisato Kondoh[b], Makoto Furutani-Seiki[b,*]

[a]*Department of Physiological Chemistry, Graduate School of Pharmaceutical Sciences, University of Tokyo, Tokyo 113-0033, Japan*
[b]*ERATO, Jaman Science and Technology Corporation, Kondoh Differentiation Signaling Project, Kawara-cho 14, Yoshida, Sakyo-ku, Kyoto 606-8305, Japan*
[c]*Graduate School of Biostudies, Kyoto University, Kyoto 606-8501, Japan*
[d]*Department of Applied Biological Chemistry, University of Tokyo, Tokyo 113-0033, Japan*
[e]*Graduate School of Frontier Biosciences, Osaka University, Osaka 565-0871, Japan*
[f]*Division of Experimental Immunology, Institute for Genome Research, The University of Tokushima, Tokushima 770-8503, Japan*
[g]*Department of Molecular Medicine and Pathophysiology, Research Institute, Osaka Medical Center for Cancer and Cardiovascular Diseases, Osaka 537-8511, Japan*
[h]*Developmental Biology Programme, EMBL Heidelberg, Meyerhofstrasse 1, D-69117, Heidelberg, Germany*

Received 20 January 2004; received in revised form 30 March 2004; accepted 3 April 2004

Abstract

We report here mutations affecting various aspects of liver development and function identified by multiple assays in a systematic mutagenesis screen in Medaka. The 22 identified recessive mutations assigned to 19 complementation groups fell into five phenotypic groups. Group 1, showing defective liver morphogenesis, comprises mutations in four genes, which may be involved in the regulation of growth or patterning of the gut endoderm. Group 2 comprises mutations in three genes that affect the laterality of the liver; in *kendama* mutants of this group, the laterality of the heart and liver is uncoupled and randomized. Group 3 includes mutations in three genes altering bile color, indicative of defects in hemoglobin–bilirubin metabolism and *globin* synthesis. Group 4 consists of mutations in three genes, characterized by a decrease in the accumulation of fluorescent metabolite of a phospholipase A_2 substrate, PED6, in the gall bladder. Lipid metabolism or the transport of lipid metabolites may be affected by these mutations. Mutations in Groups 3 and 4 may provide animal models for relevant human diseases. Group 5 mutations in six genes affect the formation of endoderm, endodermal rods and hepatic bud from which the liver develops. These Medaka mutations, identified by morphological and metabolite marker screens, should provide clues to understanding molecular mechanisms underlying formation of a functional liver.
© 2004 Elsevier Ireland Ltd. All rights reserved.

Keywords: Liver development; Medaka; Hepatoblast; Hepatic bud; Laterality; Gall bladder; Lipid metabolism; Endoderm formation; Bile; Zebrafish

1. Introduction

The liver is an organ with vital functions, including processing and storage of nutrients, maintenance of serum composition, detoxification and bile production. The major functional cells of a liver are the hepatocytes

* Corresponding authors. Tel.: +81-75-771-9362; fax: +81-75-771-3835 (M. Furutani-Seiki); Tel.: +81-3-5841-4754; fax: +81-3-5841-4751 (H. Nishina).
E-mail addresses: furutani@dsp.jst.go.jp (M. Furutani-Seiki), nishina@mol.f.u-tokyo.ac.jp (H. Nishina).

0925-4773/$ - see front matter © 2004 Elsevier Ireland Ltd. All rights reserved.
doi:10.1016/j.mod.2004.04.004

and cholangiocytes (bile duct cells). The common progenitors of hepatocytes and cholangiocytes are derived from hepatoblasts in the hepatic endoderm. The hepatic endoderm arises from the foregut endoderm that interacts with adjacent tissues, such as the cardiac mesoderm and septum transversum mesenchyme (Douarin, 1975; Grapin-Botton and Melton, 2000; Tam et al., 2003; Zaret, 2001). The vasculature is another important component of the liver. Angioblasts, which are endothelial cell precursors, accumulate around the liver bud and become interspersed with the hepatoblasts (Matsumoto et al., 2001).

Regulatory genes that are crucial for liver formation have been isolated in mice and confirmed by reverse genetics (see Zaret, 2002 for a review). For instance, we have shown using SEK1 or MKK7-deficient mice that two stress-signaling kinases, SEK1 (also called MKK4) and MKK7, play crucial roles in hepatoblast proliferation and survival (Nishina et al., 1999; Wada et al., 2004; Watanabe et al., 2002). Although a reverse genetic approach is powerful in characterizing functions of known genes, knowledge of genes, particularly in hepatic bud formation from endoderm, morphogenesis and laterality of the liver, and hemoglobin–bilirubin or lipid metabolism, is still limited. Therefore, identifying mutations affecting these aspects of liver formation and function will uncover genes required for these processes.

Systematic forward genetic screens for mutations affecting embryogenesis have been carried out in zebrafish. Zebrafish embryos are transparent and sustain defects in circulation or hematopoiesis, because oxygen supplied by simple diffusion is sufficient for development and the liver is not the site of embryonic hematopoiesis (Alexander and Stainier, 1999). These characteristics of zebrafish have enabled the study of genes involved in the development of endoderm, cardiovascular and hematopoietic systems. Zebrafish mutants with impaired endoderm formation, degenerative liver, impaired lipid metabolism in the intestine and hepatobiliary system, have been identified (Chen et al., 1996; Farber et al., 2001; Pack et al., 1996; Schier et al., 1996, 1997; Zhang et al., 1998). Furthermore, the availability of transgenic lines expressing GFP throughout the digestive system allows direct observation of the endoderm and digestive organ formation in living embryos (Field et al., 2003; Ober et al., 2003). However, genes identifiable in a single model organism by the mutational approach are limited due to a functional overlap of genes in vertebrates.

Medaka is evolutionally distant from zebrafish and interspecies differences in the functional overlap of genes allow identification of mutations as yet unidentified in zebrafish. The liver and gall bladder are more conspicuous in living embryos in Medaka than in zebrafish. Medaka has a smaller genome size (half that of zebrafish, and only double that of Fugu), inbred strains are available, and a wide range of growth temperatures facilitates identification of temperature sensitive mutations.

Taking advantage of these attributes of Medaka, we have carried out a mutagenesis screen, using multiple assays to detect defects in various aspects of the development of a functional liver. These include not only morphological assays, but also those of the functions related to the liver, such as hemoglobin–bile and lipid metabolism. In this report, we present the initial characterization of mutations isolated in the screen, ranging from those affecting endoderm formation to those affecting liver physiology in Medaka.

2. Results

2.1. Designing of mutant screening based on multiple criteria

2.1.1. Morphological screening

We carried out the morphological screen of the liver by inspecting live embryos when the liver became discernible from 4 days post-fertilization (dpf, stage (st.) 32) at 28 °C and the gall bladder became prominent at approximately 120 h post-fertilization (hpf, st. 36). The lateral views of wild-type embryos and livers at st. 32 and 36 are shown in Fig. 1A–C. The liver, gall bladder, and blood vessel from the liver connected to the Cuvierian duct developing on the left side of the embryo were observed (Fig. 1B,C).

To analyze the time course of liver development, we carried out in situ hybridization between st. 21 and 39 using endoderm-specific markers, *foxA3* and *gata6* (Fig. 1D–P). The hepatic bud formed from the endoderm rod in wild-type Medaka at st. 25 (Fig. 1H,I). At st. 27 the liver began to enlarge and the swim bladder appeared from the gut tube and began to enlarge (Fig. 1J–P, arrowheads and asterisks indicate the liver and swim bladder, respectively). *foxA3* was also expressed in the pharynx, but unlike in zebrafish, *foxA3* was not expressed in the pancreas in Medaka (data not shown). On the other hand, the expression of *gata6* was restricted to the liver from st. 25 to 31 (Fig. 1I,K,M). Soon after at st. 31, we screened live embryos. No expression of *gata6* was detected in the liver at st. 34 (Fig. 1O). In zebrafish, *gata6* is expressed in the liver and gut. Thus, the expression pattern of *gata6* in Medaka is different from that in zebrafish.

Considering the relatively late development of the liver in embryogenesis, care was taken to avoid isolating mutants showing a general retardation of development. Mutants with altered liver morphologies, such as the size, shape, and laterality of livers, were screened first at st. 32 and confirmed at st. 36 when the liver and gall bladder became larger in wild-type embryos.

2.1.2. Screening of gall bladder color

Based on the assumption that impaired bile metabolism in the liver results in an abnormal color of bile, we inspected

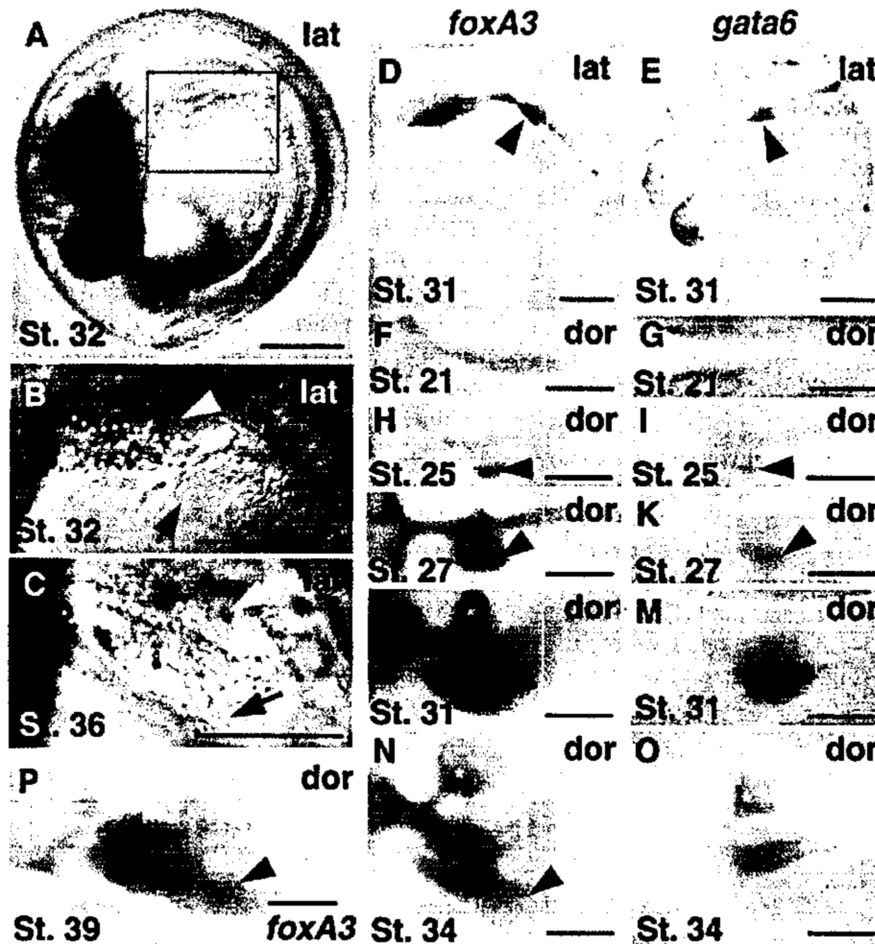

Fig. 1. Liver development in Medaka. Live (A–C) and fixed wild-type embryos stained by in situ hybridization using the *foxA3* (D, F, H, J, L, N, and P) and *gata6* (E, G, I, K, M, and O) probes. (A–C, D, and E) Lateral view; (F–P) Dorsal view. (A–C) The liver was readily visible from the left side of living embryos at st. 32 (A and B) and st. 36 (C) when screening was carried out; (F and G) st. 21; (H and I) The hepatic bud was formed at st. 25 and subsequently liver growth occurred; (J and K) st. 27; (L and M) st. 31; (N and O) st. 34 and (P) st. 39. White broken line demarcates the liver. White arrowheads and black arrows indicate the gall bladder and the vein of the liver, respectively. Black arrowheads and white asterisks show the hepatic bud and the liver, and the swim bladders, respectively. lat: lateral, dor: dorsal. Scale bars correspond to 200 μm.

color of bile in the gall bladder. Bile in the wild-type embryo at st. 35 was light green. Impaired erythropoiesis was reported to alter bile color in zebrafish (Shafizadeh et al., 2002). To distinguish mutations affecting erythropoiesis from those affecting bile metabolism in the liver, we carried out hemoglobin staining with *o*-dianisidine and in situ hybridization analysis using embryonic globins such as *α-0*, *α-1*, and *β-1 globins*.

2.1.3. Screening using fluorescent phospholipid reporters

We used a fluorescent phospholipid reporter, PED6, to screen for mutations affecting lipid metabolism (Farber et al., 2001).

PED6 is a synthetic substrate for PLA_2 that becomes fluorescent after cleavage in the intestine and its fluorescent PED6 metabolites undergo rapid hepatobiliary transport, labeling the liver before the gall bladder, as shown in Fig. 5C. Embryos administered with PED6 showed intense fluorescence in the gall bladder, liver and intestinal lumen. We screened for embryos showing an impaired accumulation of the fluorescent metabolites of PED6. To exclude mutations affecting the swallowing of PED6, the unquenched form of PED6, BODIPY-FL-C5, was used.

2.1.4. Rescreening for mutations affecting early embryogenesis using the foxA3 probe

In addition to directly screening for liver associated phenotypes, we also screened for mutations affecting endoderm and hepatic bud formations among mutants that were initially identified on the basis of morphological abnormalities (Furutani-Seiki et al., 2004). To this end, we carried out in situ hybridization using *foxA3* at st. 28 (Fig. 1J).

2.2. Mutations affecting formation and function of the liver isolated by the multi-assay screen

By screening 210 F2 families, we have isolated 19 mutations. Since all of the mutations were zygotic recessive mutations, mutants refer to homozygotes of these mutations in this report. These mutations were classified into the following five phenotypic groups and features of these mutations were summarized in Table 1.

2.2.1. Mutations affecting liver morphogenesis

Mutations in four genes, *kakurembo* (*kak*), *hiohgi* (*hio*), *origami* (*ora*) and *kamifusen* (*kam*) affect liver morphology.

In live *kak* embryos at st. 34, the liver was not clearly discernible at the position where it should be formed and the gall bladder was dislocated anteriorly (Fig. 2A,B). In *kak* mutant embryos at st. 24, the expression level of *gata6* in the liver markedly reduced, while that of *cardiac myosin light chain* (*mlc*) in the heart was unaltered (Fig. 2G,H). In *kak* mutant embryos at st. 34, the expression level of *foxA3* was also greatly reduced (Fig. 2I,J). Since liver budding appeared to occur in *kak* mutants, *kak* may be required for the growth or maintenance of the liver. The gut tube was undulated at st. 36 (data not shown) without affecting the epithelial structure of the gut tube (Fig. 2N,O,Q,R).

In *hio* mutant embryos at st. 36 and at later stages, the liver was small and malformed (Fig. 2C,D, and data not shown). In situ hybridization using the *gata6* probe clearly showed impaired liver formation in *hio* mutant embryos at st. 30 (Fig. 2K,L). In addition to the liver defects, *hio* mutant embryos also lacked pectoral fins and died after hatching.

In *kam* mutant embryos, blood accumulated in the liver, and the liver was malformed (Fig. 2E). The expression of *gata6* appeared normal (Fig. 2M).

In *ora* mutant embryos at st. 36, the liver shape was altered, the gall bladder was displaced and the gut undulated (Fig. 2F). *ora* mutant embryos at st. 40 have an enlarged swim bladder and undulated gut, whereas the heart and kidneys appeared unaltered (Fig. 2T,U). Cross sections at the level of the liver, gut tube, and yolk showed that hepatocytes seemed normal, but the embryo itself lay apart from the yolk and the intestine was malformed (Fig. 2P,S). In contrast to regularly aligned polarized epithelial cells in

Table 1
Mutations affecting liver formation and function

Genes	Alleles	Viability	Phenotypes	Other phenotypes	References
Group 1: Mutations affecting liver morphogenesis					
kakurembo (kak)	*j140-3B*	Embryonic lethal	Small and mislocated liver	Mislocated gall bladder, undulated gut	
hiohgi (hio)	*j102-5B*	Embryonic viabe	Small liver	Fin missing	
kamifusen (kam)	*j124-4A*	Embryonic lethal	Malformed liver	Blood accumulated near the liver	
origami (ora)	*j137-1A*	Embryonic viable	Malformed liver	Undulated gut, enlarged swim bladder	
Group 2: Mutations affecting liver laterality					
kendama (ken)	*j103-11C*	Develop to adult fish	Inverted positions of liver and gall bladder	Medially located liver and missing spleen	
hanetsuki (hat)	*j68-7A*	Develop to adult fish	Inverted positions of liver and gall bladder	Inverted heart looping	
dendendaiko (den)	*j73-11A*	Develop to adult fish	Inverted positions of liver and gall bladder	Inverted heart looping	
Group 3: Mutations affecting bile color in the gall bladder					
akane (aka)	*j140-8A*	Embryonic lethal	Deep red bile	Colorless erythrocytes	
suou (suo)	*j98-5A*	Adult viable	Light red bile	Erythrocytes were faint red	
ominaeshi (omi)	*j24-13E*	Embryonic lethal	Colorless bile	Colorless erythrocytes	
Group 4: Mutations affecting lipid metabolism					
ukon (uko)	*j152-8A*	Embryonic lethal	Failure in metabolizing PED6	Edematic after hatching	a
aonibi (aon)	*j60-3A/j9-2F*	Embryonic lethal	Failure in metabolizing PED6	Small and degenerated forebrain at st. 38	
uguisucha (ugu)	*j153-9A*	Embryonic lethal	Failure in metabolizing PED6	Growth retardation after hatching	
Group 5: Mutations affecting endoderm formation					
akatsuki (aku)	*j22-15A/jf121-1A*	Embryonic lethal	Lacking *foxA3* expression	Similar to the zebrafish *oep* phenotype	a,b
akebono (ake)	*j54-7A*	Embryonic lethal	Lacking *foxA3* expression	Similar to the zebrafish *oep* phenotype	a,b
mochizuki (moc)	*j96-11B*	Embryonic lethal	Lacking *foxA3* expression	Similar to the zebrafish *oep* phenotype	a,b
sakura (sak)	*jr10-4A/j153-3A*	Embryonic lethal	Lacking the hepatic bud	Loss of heart and degeneration of eyes	b
hirame (hir)	*j54-20C*	Embryonic lethal	Defect in hypoblast convergence	Flat embryo	a,b
fukuwarai (fku)	*j8-33A/j93-4A*	Embryonic lethal	Lacking the hepatic bud	Cell polarity and alignment affected	a,b

References: a, Kitagawa et al., 2004; b, Furutani-Seiki et al., 2004.

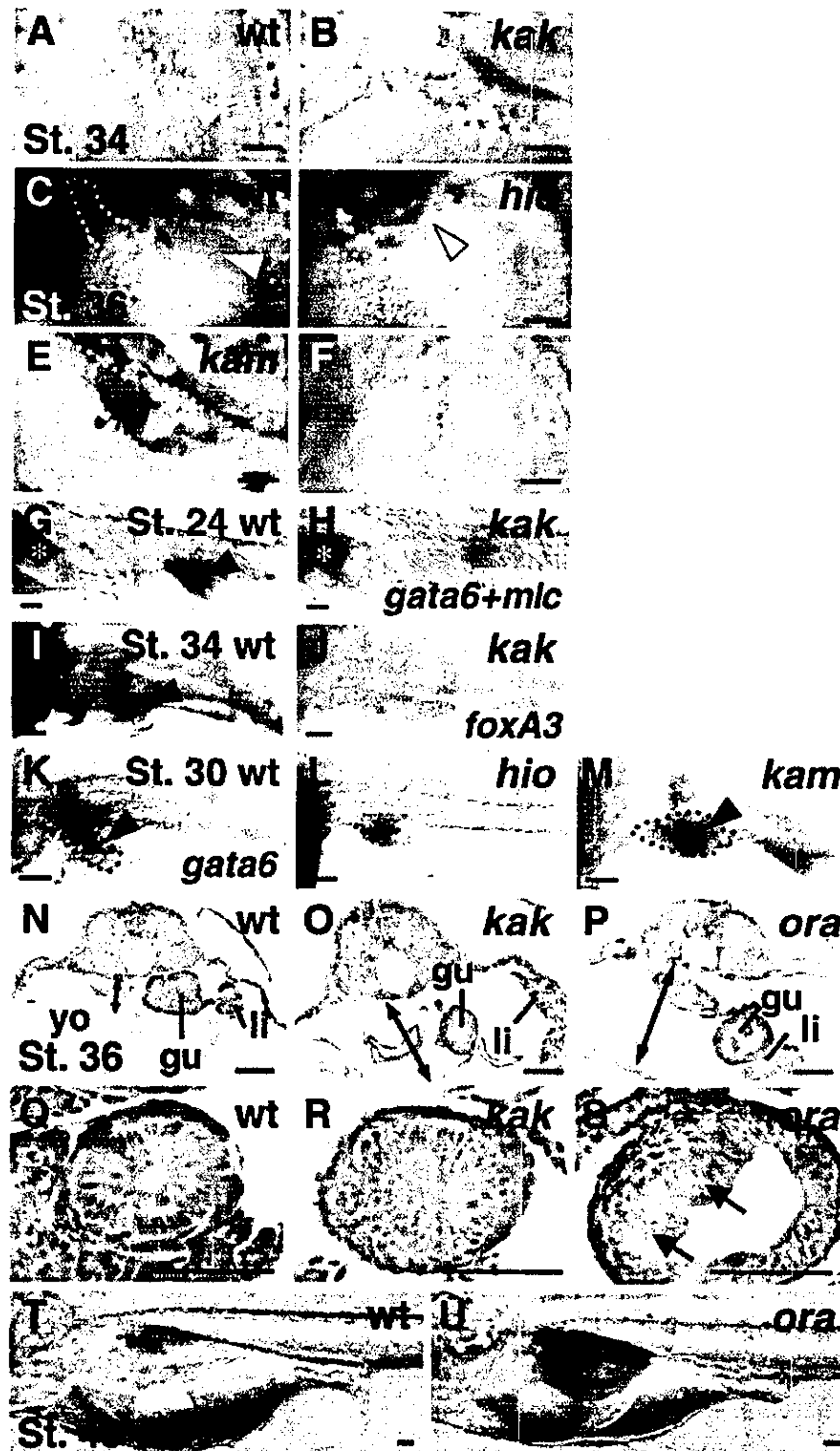

Fig. 2. *kak, hio, kam* and *ora* mutations affect liver morphogenesis. (A–F, T, and U) Live embryos; (G–M) Fixed embryos stained by in situ hybridization; (N–S) Histological sections stained with hematoxylin and eosin. in situ hybridization was performed using the probes of (G and H) *gata6* and *mlc*; (I and J) *foxA3*; and (K–M) *gata6*. (Q–S) Enlarged view of (N–P), respectively. (A–F, K–M, T and U) Lateral views, (G and H) dorsal views, anterior to the left, (N–S) Cross-sections. (A and B) st. 34; (C–F) st. 36; (G and H) st. 24; (I and J) st. 34; (K–M) st. 30; (N–S) st. 36; (T and U) st. 40. (A, C, G, I, K, N, Q, and T) Wild-type sibling embryos; (B, D, F, H, J, L, M, O, P, R, S, and U) Mutant embryos of (B, H, J, O, and R) *kak*; (D and L) *hio*; (E and M) *kam*; (F, P, S, and U) *ora*. Both arrows indicate the space between the yolk and the embryo proper. White broken lines demarcate the liver. Black and white arrowheads and white asterisks indicate the hepatic bud, gall bladder, and heart, respectively. Black arrows indicate the affected epithelial structure of the gut in the *ora* mutant. Gu: gut, Li: liver, yo: yolk. Scale bars correspond to 50 μm.

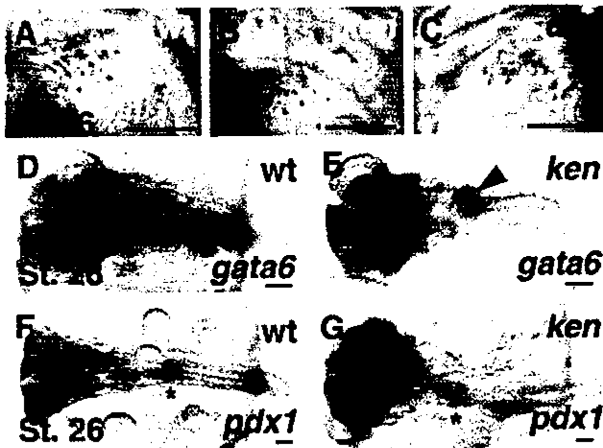

Fig. 3. *ken* and *den* mutations affect liver laterality. (A–C) Live embryos; (D–G) Embryos stained by in situ hybridization using the *gata6* (D and E) and *pdx1* (F and G) probes. (A–C) Lateral views, (D–G) dorsal views, (A, B, D–G) anterior to the left, (C) anterior to the right. (A and D) Wild-type sibling embryos; (B, C, E, and G) Mutant embryos, (B and E) *ken*, (C) *den* mutant embryos. White broken lines demarcate the livers. Black arrowheads, white arrowheads, and black asterisks indicate the liver, gall bladder, and pancreas, respectively. Scale bars correspond to 150 μm.

wild-type embryos, epithelial cells were irregularly arranged in *ora* mutant embryos (arrows in Fig. 2S).

2.2.2. Mutations affecting liver laterality

Mutations in three genes, *kendama* (*ken*), *dendendaiko* (*den*) and *hanetsuki* (*hat*), caused altered liver laterality (Fig. 3). In addition to the liver, the gall bladder, hepatic vein and blood vessels from the liver to the Cuvierian duct were also inverted in these mutant embryos. All mutant embryos hatched and their larvae swam well, suggesting that the altered laterality of the liver and other organs do not affect embryonic viability.

In *ken* mutant embryos, the laterality of the liver and heart was found to be uncoupled, as shown in Table 2. *ken* mutant embryos are classified into four groups according to the location of the liver and heart: (1) the liver shifts to the center and the heart is normally located, L(c)H(n); (2) the liver shifts to the center and the heart was inverted, L(c)H(i); (3) the liver shifts to the right with the heart normally positioned, L(r)H(n); (4) the liver shifts to the right and the heart was inverted, L(r)H(i). These phenotypes were observed in subsequent generations. A *ken* mutant embryo of L(c)H(n) at st. 36 is shown in Fig. 3B. In the embryo in which the liver and gall bladder were located at the center of the body, the liver was not visible from the left view but the heart was observed at the normal location (data not shown). Since, in Medaka the pancreas, detected by the expression of *pdx1*, lies at the center of embryos in the wild-type embryo at st. 26 (Assouline et al., 2001), we could not determine the laterality of the pancreas in *ken* mutant embryos (Fig. 3F,G).

In *den* and *hat* mutant embryos, the liver, gall bladder, and the heart were all inverted in these mutants, as shown in Fig. 3C and Table 2. These results suggest that while *den* and *han* are required for the general laterality of the body, *ken* is required for coupling the laterality of the liver and heart.

2.2.3. Mutations affecting color of bile in the gall bladder

Mutations in three genes, *suou* (*suo*), *akane* (*aka*) and *ominaeshi* (*omi*), affected the color of bile in the gall bladder (Fig. 4). Bile in the wild-type embryo at st. 35 was light green, as shown in Fig. 4A. The bile colors in the three mutants, *suo*, *aka* and *omi*, were orange, deep red and white, respectively (Fig. 4B–D). *aka* and *omi* mutant embryos were embryonic lethal, but *suo* mutant embryos hatched and *suo* homozygotes were fertile.

To determine whether these mutations affect either erythropoiesis or hemoglobin-bile metabolism, we first carried out hemoglobin staining with *o*-dianisidine. As shown in Fig. 4E–H, the blood vessels and heart, but not the gall bladder, were stained in *suo* mutant embryos, but were not stained in *aka* and *omi* mutant embryos. We next examined the expression of *globin* genes by in situ hybridization. Medaka embryos express three types of *globin*, *α-0*, *α-1*, and *β-1* (Maruyama et al., 2002). *α-0*, *α-1*, and *β-1 globins* were expressed in *suo* mutants at st. 33 (Fig. 4I,J,M,N, and data not shown), whereas *α-0*, but not *α-1* and *β-1 globins* were expressed in *aka* mutant embryos (Fig. 4K,O, and data not shown). None of *α-0*, *α-1*, and *β-1 globins* were expressed in *omi* mutant embryos (Fig. 4L,P, and data not shown). These results indicate that *aka* and *omi* mutations affect erythropoiesis. On the other hand,

Table 2
Frequency of alteration of liver and heart laterality

		Laterality phenotype (%)						
		Total	L(l) H(n)	L(l) H(i)	L(c) H(n)	L(c) H(i)	L(r) H(n)	L(r) H(i)
ken	mut	39	0	0	10 (26)	16 (40)	3 (7)	10 (26)
	sib	102	101 (99)	1 (1)	0	0	0	0
hat	mut	21	0	0	0	0	0	21 (100)
	sib	96	95 (99)	1 (1)	0	0	0	0
den	mut	19	0	0	0	0	1 (6)	18 (94)
	sib	120	119 (99)	1 (1)	0	0	0	0

L, liver; H, heart; l, left; c, center; r, right; n, normal; i, invert.

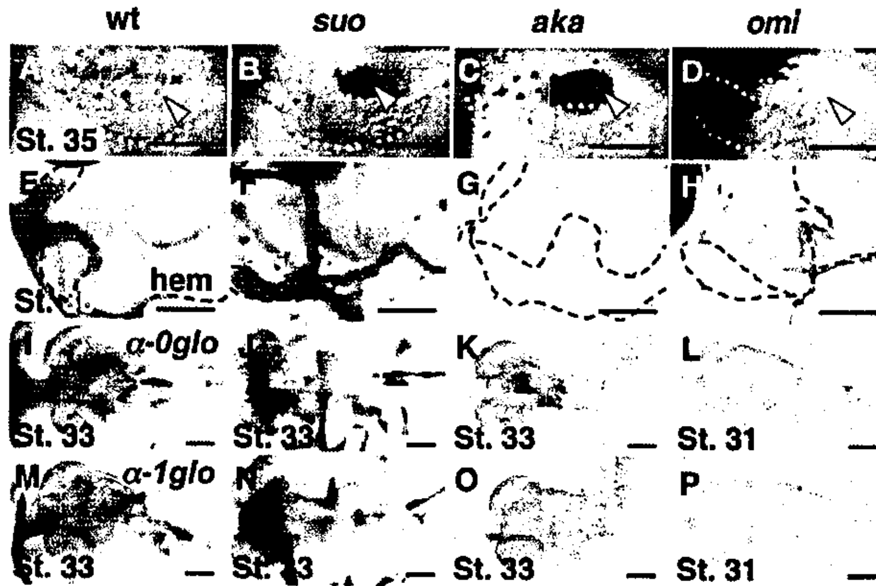

Fig. 4. *aka*, *suo* and *omi* mutations affect bile color. (A–D) Live embryos; (E–H) Hemoglobin staining; (I–P) in situ hybridization, using (I–L) the *α-0 globin*, and (M–P) *α-1 globin* probes. (A–D) st. 35; (E–H) st. 36; (I–K, M–O) st. 33 and (L and P) st. 31. (A, E, I, and M) wild-type sibling embryos, (B, F, J, and N) *suo*, (C, G, K, and O) *aka* and (D, H, L, and P) *omi* mutant embryos. White arrowheads and white broken lines indicate the gall bladder and margin of the liver, respectively. Black broken lines show the Cuvierian duct. Black to brownish spots are melanophores on the yolk. Scale bars correspond to 200 μm.

erythropoiesis appears normal and orange bile in the gall bladder is not due to the accumulation of erythrocytes in *suo* mutant embryos, suggesting that *suo* mutation may affect hemoglobin–bilirubin metabolism.

2.2.4. Mutations affecting lipid metabolism

The fluorescence intensities of PED6 metabolites markedly decreased in three mutant embryos, *ukon* (*uko*), *aonibi* (*aon*) and *uguisucha* (*ugu*), at st. 35 (Fig. 5C–F). To examine whether the decrease in fluorescence intensity is due to the inability of swallowing PED6, we loaded the three mutant embryos with BODIPY-FL-C5, an unquenched form of PED6. All the mutants swallowed the unquenched form of PED6, and the gut, liver and gall bladder showed fluorescence as wild-type embryos (Fig. 5G–J).

uko and *aon* mutant embryos appeared normal in the morphologies of the liver, gall bladder and intestine at st. 35 as shown in Fig. 5B, and *ugu* mutant embryos started to show retardation in development from st. 35 (data not shown). *uko* mutant embryos could hatch but their larvae died a few days after hatching (data not shown). Both *aon* and *ugu* mutant embryos were embryonic lethal. The forebrain was reduced in size from st. 23 in *aon* mutant embryos (Kitagawa et al., 2004). These results suggest that the *uko*, *aon* and *ugu* genes are required for the metabolism or transport of lipids in the hepatobiliary system.

2.2.5. Mutations affecting patterning of endoderm

Six mutations affecting formation of the endodermal rod and/or hepatic bud were identified. Mutations in the *fukuwarai* (*fku*) genes affected endodermal rod morphogenesis (Fig. 6G). Although in *fku* mutant embryos *foxA3* was expressed in the pharynx, hepatic region and the gut (Fig. 6, open circle, arrow head and asterisk, respectively), parts of the endodermal rod were randomly dislocated (Fig. 6G arrow) as other epithelial structures, such as the head structures originated from neuroepithelium (Fig. 6B closed arrow, Kitagawa et al., 2004).

In *sakura* (*sak*) mutant embryos, *foxA3* was expressed in the gut and hepatic region, but not in the pharynx (Fig. 6H). Growth of the hepatic region appeared to be affected and anterior part of the endodermal rod may be missing or misspecified. In *sak* mutant embryos, the heart was not formed and the eyes became degenerated at st. 28 (Fig. 6C, closed arrow).

In embryos with mutations in three genes, *akatsuki* (*aku*), *akebono* (*ake*) and *mochizuki* (*moc*), the endodermal rod was missing (Fig. 6I, data not shown). These mutants exhibited a body patterning phenotypes similar to those of *one-eyed-pinhead* (*oep*) zebrafish mutants (Fig. 6D, data not shown, Kitagawa et al., 2004). While embryos with mutations in only one gene exhibit the *oep* mutant phenotypes, those in three genes display similar phenotypes in both body patterning and endoderm formation.

In *hirame* (*hir*) mutant embryos, *foxA3* expressing endodermal cells did not converge properly, affecting the endermal rod formation (Fig. 6J open arrow). *hir* mutant embryos were flat and tissues such as the lens and heart were mislocated (Fig. 6E, the closed arrow indicates mislocated lens, Kitagawa et al., 2004).

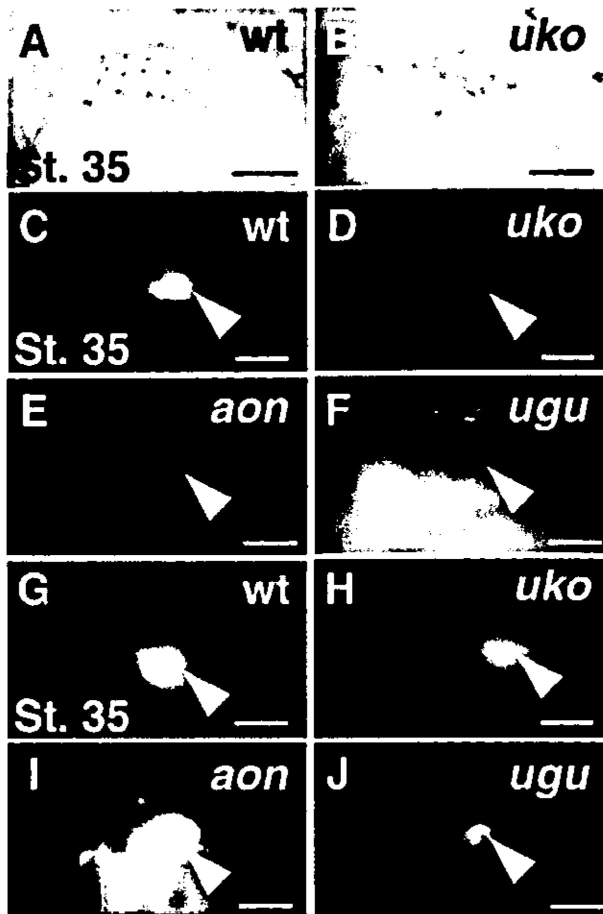

Fig. 5. *uko*, *ugu*, and *aon* mutations affect lipid metabolism. Laterl view, anterior to the left. Live embryos of unstained (A, B), stained with PED6 (C–F) and BODIPY FL-C5 (G–J) at st. 35. (A, C, and G) Wild-type, (B, D, and H) *uko*, (E and I) *aon* and (F and J) *ugu*. Metabolized PED6 (C-F) or BODIPY FL-C5 (G–J) can been seen as a green emission (Em: 505 nm) in the gall bladder (white arrowheads). White broken lines demarcate the margin of the liver. Scale bars correspond to 200 μm.

3. Discussion

3.1. Screening for mutations affecting liver development in Medaka

Partly due to the functional overlap of genes, particularly in vertebrates, mutagenesis screens in a single species are unlikely to be sufficient for identifying all essential genes involved in a particular biological process Therefore, mutagenesis screens and analyses of Medaka mutants complement those in zebrafish, in identifying a wider repertoire of genes by a forward genetic approach in vertebrates.

Our mutagenesis screen in Medaka identified mutations in 19 genes affecting various aspects of the development of the liver and associated tissues. These mutations are classified into five groups: (1) mutations affecting liver morphogenesis; (2) mutations affecting liver laterality; (3) mutations affecting of bile color; (4) mutations affecting lipid metabolism; and (5) mutations affecting endoderm and hepatic bud formation. In zebrafish, a mutagenesis screen using GFP-transgenic fish, whose developing endoderm or organs arising from endoderm are more conspicuous, is underway (D. Y. R. Stainier, personal communication). Thus, mutagenesis screens in both Medaka and zebrafish should be complementary in identifying conserved and divergent mechanisms of liver development.

In our screen, we initially aimed to identify mutations affecting formation and function of the liver specifically. To this end we carried out a screen by multiple criteria to reveal the specificity of the defect. Majority of mutations that we identified were those affecting tissues in addition to the liver during development. From these results, we deduced that mutations affecting the liver specifically may be very limited and that even if defects are not confined to the liver, mutated genes are important for the formation of the liver or physiological functions in which the liver is involved. Thus expression of these genes identified in our screen may not be restricted to the liver but to the tissues, from which the liver originates or those working with the liver to exert its physiological functions.

3.2. Mutations affecting liver morphogenesis

Several explanations may account for the phenotypes of Group 1 mutants with defects in the liver, and gall bladder and gut. First, cell-autonomous defects may affect the regional morphogenesis of the endodermal rod, resulting in altered morphologies of the liver, gall bladder and gut. Second, non-cell-autonomous defects such as the interaction between the surrounding lateral mesoderm and endodermal rod may cause the phenotype. Third, there may be regulatory interactions among the hepatic bud, primordium of the gall bladder and the intestinal bulb. Transplantation experiments to determine the cell autonomy of these mutations would be useful to clarify these possibilities. Finally, since nutrients absorbed from the intestine are metabolized in the liver (Wallace and Pack, 2003; Warga and Stainier, 2002), a defect in the intestine may affect liver growth. The idea that the timing of liver growth is dependent on nourishment from the intestine needs to be further investigated.

In *kak* mutants, although the hepatic bud is formed, the liver is very small at st. 34 and the gall bladder may have shifted its position due to the small liver. This suggests that *kak* is required for the formation of the liver from the hepatic bud.

In *hio* mutants, the liver is small and malformed and the pectoral fin is missing. In zebrafish, some mutations affect the pectoral fin, but no mutations have been reported to affect both the liver and pectoral fin yet (Grandel and Schulte-Merker, 1998; Neumann et al., 1999; van Eeden et al., 1996). It has been suggested that, however, mesodermal components or FGF signaling is

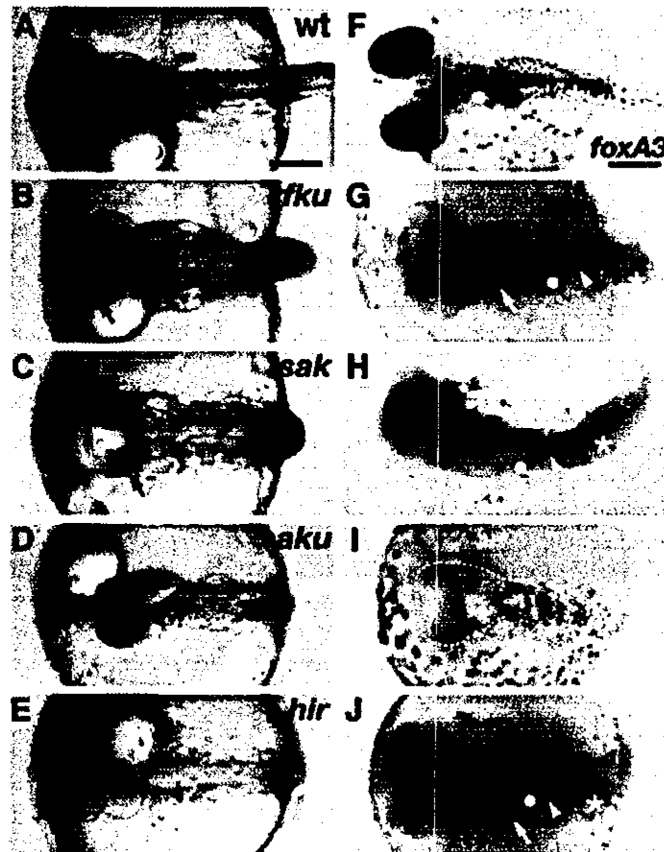

Fig. 6. *fku*, *sak*, *aku*, and *hir* mutations affect patterning of endoderm. Dorsal views of (A–E) live embryos and (F–J) embryos stained by in situ hybridization using the *foxA3* probe at st. 28. (A and F) Wild-type embryos, (B and G) *fku*; (C and H) *sak*, (D and I) *aku* and (E and J) *hir* mutant embryos. Open circle, arrowhead, and asterisk indicate the sites where pharynx, hepatic bud, and the gut are normally formed, respectively. Closed arrows show dislocated head structure in B, degenerating eye in C, dislocated lens in E. Open arrows indicate mislocated part of the endodermal rod in G and *foxA3* positive cells inappropriately converged in J. The margin of the embryo was demarcated by the broken line in I. Scale bars correspond to 250 μm.

required for the formation of the pectoral fin and liver (Fischer et al., 2003; Jung et al., 1998; Martin, 1998). It would be interesting to examine mesoderm development and FGF expression in *hio* mutant embryos to further characterize this mutation.

In *kam* mutant embryos, in addition to a malformed liver and gall bladder, the heart is small and blood accumulates near the liver and gut. Such blood accumulation may reflect a defect either in vasculature formation in the liver or in endothelial cell development. In *vegfr2/flk-1* mutant mice with endothelial cell defects, liver budding does not occur. However, in zebrafish, although *cloche* zebrafish mutants lacking all endothelial cells, normal liver budding and development occurs (Field et al., 2003; Stainier et al., 1995). However, severe cardiac edema did not allow analysis of the requirement of endothelial cells during the growth of the liver in those studies. In *kam* mutants, liver budding seems to occur normally, but the growth of the liver may be affected. Detailed analysis of *kam* mutants at the budding and growth periods using endothelial markers would be useful for the further characterization of this mutation.

3.3. Laterality of the liver and other organs

The laterality of all the organs is inverted in most of mutants of zebrafish and mice (Essner et al, 2000; Faucourt et al., 2001; Mochizuki et al., 2002; Schilling et al., 1999), but there are a few reports on uncoupled laterality of the organs (Bisgrove et al., 2000; Field et al., 2003). In zebrafish *flh* and *boz* mutants, the laterality of the liver and heart is randomized and uncoupled (Chin et al., 2000). *flh* is required for specification of the chordamesoderm and *boz* is required for dorsal axis formation. Both *flh* and *boz* are required for early specification of the notochord. Collectively, *ken* mutants show a defect in the laterality of the viscera as observed in *flh* and *boz* mutants but do not show other morphological deficits. An interesting possibility is that *ken* might be a component of the signaling downstream of *boz* and *flh*.

3.4. Mutations affecting bile color

Since a compromised function of the liver readily results in jaundice in human, hemoglobin metabolism producing bilirubin is one of the most important functions of the liver

Hereditary diseases affecting bilirubin metabolism are known in human (Nowicki and Poley, 1998).

Mutations affecting the color of bile in the gall bladder and red blood cells were identified in zebrafish (Ransom et al., 1996; Shafizadeh et al., 2002; Thisse and Zon, 2002; Weistein et al., 1996). *aka* and *omi* mutations also affect erythropoiesis in Medaka. In contrast, *suo* mutation seems to be the first mutation affecting hemoglobin–bilirubin metabolism in zebrafish and Medaka. It would be of interest if *suo* mutation models a human disease.

3.5. Lipid metabolism

PED6 is a substrate for PLA_2 cleavage and a sensitive reporter of its enzymatic activity in vivo (Farber et al., 2001). PLA_2 is important in the generation of lipid signaling molecules, host defenses, lipid absorption and cancer. It is thus a good chemical reagent for screening mutations affecting lipid metabolism. Using PED6, four mutations affecting digestive organ morphology and one mutation affecting bile synthesis or secretion were identified in zebrafish (Farber et al., 2001).

The *uko, aon,* and *ugu* mutations may affect steps in the lipid metabolism pathway, such as ingestion and cleavage of the lipid within the intestine, and subsequent hepatobiliary transport to the gall bladder (Faber et al., 2001). Further biochemical characterization is necessary to determine which component of lipid metabolism is affected in Group 4 mutants.

3.6. Mutations affecting endoderm formation and patterning

The phenotypes of *aku, ake* and *moc* mutants in patterning of the body, endoderm and mesoderm, are similar to those of zebrafish *oep* mutants with defects in the Nodal signaling pathway (Schier et al., 1996, 1997; Zhang et al., 1998). Zebrafish mutations in other components of the Nodal signaling pathway, such as *cyclops, squint* and *smalspur*, exhibit phenotypes substantially different from that of *oep* mutation (Brand et al., 1996). Cloning of three genes, *aku, ake* and *moc* genes will clarify the conserved or divergent functions of these genes in endoderm specification.

The *fku* and *hir* mutants show unique phenotypes in the patterning of the body, not recorded yet in the collection of zebrafish mutants. In *fku* mutants, parts of the head, such as the eyes and nose, are mislocated. In *hir* mutants, the body becomes thinner and several tissues, such as the lens and heart, are mislocated. Although the endodermal cells expressing *foxA3* are present, morphogenesis of the hepatic bud and convergence of the endodermal cells did not occur properly in *fku* and *hir* mutants, respectively. Interestingly, the common feature between *fku* and *hir* mutants is the marked defect of cell alignment in the epithelium (Furutani-Seiki et al., unpublished results). Further analysis of *fku* and *hir* mutants using early hepatocyte markers may help clarify the relationship between endodermal epithelialization and morphogenesis or specification of the endodermal rod.

In *sak* mutants, the heart primordium and the anterior part of the endodermal rod are not formed. It has been reported that the cardiac mesoderm is necessary for the induction of hepatic bud in mice (Duncan, 2003; Jung et al., 1999; Rossi et al., 2001). Further investigation of the requirement of *sak* in the heart or liver by transplantation experiments may provide insights into tissue interactions in heart and liver development.

4. Experimental procedures

4.1. Maintenance of fish stocks

Fish maintenance and mating were carried out as described elsewhere (Furutani-Seiki et al., 2004). Briefly, the Kyoto-Cab sub-strain and Kaga strain were used to induce mutations in the male germline by treatment with ENU (Ethyl-Nitroso-Urea). F3 progenies homozygous for induced mutations were generated by a three generation incrossing scheme.

4.2. Screening procedures

Live F3 progenies were screened for developmental defects at st. 32 and 36 using a Leica MZ12.5 dissecting microscope. For functional screening, we used PED6, a fluorescent PLA_2-substrate dye. PLA_2 cleavage liberates the BODIPY-acyl chain of PED6, resulting in unquenching and green fluorescent emission as described previously (Farber et al., 2001). As the control, BODIPY FL-C5, an unquenched form of PED6 was used. Embryos at st. 35 were placed in 0.5 ml of 1 × Balanced Salt Solution (BSS; 110 mM NaCl, 5 mM KCl, 1 mM $CaCl_2$, and 2.2 mM $MgSO_4$, pH 7.2), containing 0.3 μg/ml PED6 or 0.2 μg/ml BODIPY-FL-C5, and incubated in the dark for 4 h at 28 °C. The embryos were then rinsed with 1 × BSS and placed in a glass depression slide. Using a Zeiss Axioplan 2 microscope, samples were examined for fluorescence from PED6 or BODIPY-FL-C5.

4.3. Histological sections

Embryos were dechorionated and fixed in 4% paraformaldehyde in PBS(−) overnight at 4 °C. The embryos were dehydrated with ethanol and stored at −20 °C. For sectioning, they were incubated in xylene and embedded in paraffin at 67 °C. Paraffin embedded embryos were sectioned (4 μm thickness) and stained with hematoxylin and eosin.

4.4. In situ hybridization

Whole mount in situ hybridization was performed as described elsewhere (Sasado et al., 2004), using an

anti-sense DIG-labeled riboprobe generated from Medaka *foxA3*, *gata6*, *mlc*, *pdx1*, *α-0*, *α-1*, and *β-1 globin* cDNA. Dechorionated embryos were fixed with 4% paraformaldehyde and 0.1% Tween 20 in PBS(−). Embryos later than st. 30 were treated with proteinase K and to remove pigmentation, with H_2O_2. Embryos were photographed using a Leica dissecting microscope.

4.5. Whole embryo staining for hemoglobin expression

Hemoglobin staining was done as described previously (Cocca et al.. 1995). Dechorionated embryos were stained for 15 min in the dark in *o*-dianisidine (0.6 mg/ml), 0.01 M sodium acetate (pH 4.5), 0.65% H_2O_2 and 40% (vol/vol) ethanol. Stained embryos were cleared with benzyl benzoate/benzyl alcohol (2:1, vol/vol) and examined with a dissecting microscope.

Acknowledgements

We are grateful to Drs Takashi Sasaki and Noboru Nakajima for cloning *gata6* and *foxA3* probes, Dr Raphael Scharfmann for the *pdx1* probe and to Haruka Momose and Takahiro Negishi for in situ hybridization and graphical works. We would like to thank Drs Shuji Terai and Kiwamu Okita for continual discussion and encouragement. This work was supported by the ERATO project of the Japan Science and Technology Agency to H.K.

References

Alexander, J., Stainier, D.Y., 1999. A molecular pathway leading to endoderm formation in zebrafish. Curr. Biol. 9, 1147–1157.

Assouline, S., Nir, S., Lahav, N., 2001. Simulation of non-enzymatic template-directed synthesis of oligonucleotides and peptides. J. Theor. Biol. 208, 117–125.

Bisgrove, B.W., Essner, J.J., Yost, H.J., 2000. Multiple pathways in the midline regulate concordant brain, heart and gut left-right asymmetry. Development 127, 3567–3579.

Brand, M., Heisenberg, C.P., Warga, R.M., Pelegri, F., Karlstrom, R.O., Beuchle, D., Picker, A., Jiang, Y.J., Furutani-Seiki, M., van Eeden, F.J., Granato, M., Haffter, P., Hammerschmidt, M., Kane, D.A., Kelsh, R.N., Mullins, M.C., Odenthal, J., Nusslein-Volhard, C., 1996. Mutations affecting development of the midline and general body shape during zebrafish embryogenesis. Development 123, 129–142.

Chen, J.N., Haffter, P., Odenthal, J., Vogelsang, E., Brand, M., van Eeden, F.J., Furutani-Seiki, M., Granato, M., Hammerschmidt, M., Heisenberg, C.P., Jiang, Y.J., Kane, D.A., Kelsh, R.N., Mullins, M.C., Nusslein-Volhard, C., 1996. Mutations affecting the cardiovascular system and other internal organs in zebrafish. Development 123, 293–302.

Chin, A.J., Tsang, M., Weinberg, E.S., 2000. Heart and gut chiralities are controlled independently from initial heart position in the developing zebrafish. Dev. Biol. 227, 403–421.

Cocca, E., Ratnayake-Lecamwasam, M., Parker, S.K., Camardella, L., Ciaramella, M., di Prisco, G., Detrich, H.W., 1995. Genomic remnants of alpha-globin genes in the hemoglobinless antarctic icefishes. Proc. Natl Acad. Sci. USA 92, 1817–1821.

Douarin, N.M., 1975. An experimental analysis of liver development. Med. Biol. 53, 427–455.

Duncan, S.A., 2003. Mechanisms controlling early development of the liver. Mech. Dev. 120, 19–33.

Essner, J.J., Branford, W.W., Zhang, J., Yost, H.J., 2000. Mesendoderm and left-right brain, heart and gut development are differentially regulated by pitx2 isoforms. Development 127, 1081–1093.

Farber, S.A., Pack, M., Ho, S.Y., Johnson, I.D., Wagner, D.S., Dosch, R., Mullins, M.C., Hendrickson, H.S., Hendrickson, E.K., Halpern, M.E., 2001. Genetic analysis of digestive physiology using fluorescent phospholipid reporters. Science 292, 1385–1388.

Faucourt, M., Houliston, E., Besnardeau, L., Kimelman, D., Lepage, T., 2001. The pitx2 homeobox protein is required early for endoderm formation and nodal signaling. Dev. Biol. 229, 287–306.

Field, H.A., Ober, E.A., Roeser, T., Stainier, D.Y., 2003. Formation of the digestive system in zebrafish. I. Liver morphogenesis. Dev. Biol. 253, 279–290.

Fischer, S., Draper, B.W., Neumann, C.J., 2003. The zebrafish fgf24 mutant identifies an additional level of Fgf signaling involved in vertebrate forelimb initiation. Development 130, 3515–3524.

Furutani-Seiki, M., Sasado, T., Morinaga, C., Suwa, H., Niwa, K., Yoda, H., et al., 2004. A systematic genome-wide screen for mutations affecting organogenesis in Medaka, *Oryzias latipes*. Mech. Dev. 121, 647–658.

Grandel, H., Schulte-Merker, S., 1998. The development of the paired fins in the zebrafish (Danio rerio). Mech. Dev. 79, 99–120.

Grapin-Botton, A., Melton, D.A., 2000. Endoderm development: from patterning to organogenesis. Trends Genet. 16, 124–130.

Jung, J., Zheng, M., Goldfarb, M., Zaret, K.S., 1999. Initiation of mammalian liver development from endoderm by fibroblast growth factors. Science 284, 1998–2003.

Kitagawa, D., Watanabe, T., Saito, K., Asaka, S., Sasado, T., Morinaga, C., et al., 2004. Genetic dissection of the formation of the forebrain in Medaka, *Oryzias latipes*. Mech. Dev. 121, 673–685.

Martin, G.R., 1998. The roles of FGFs in the early developments of vertebrate limbs. Genes Dev. 12, 1571–1586.

Maruyama, K., Yasumasu, S., Iuchi, I., 2002. Characterization and expression of embryonic and adult globins of the teleost *Oryzias latipes* (medaka). J. Biochem. 132, 581–589.

Matsumoto, K., Toshitomi, H., Rossant, J., Zaret, K.S., 2001. Liver organogenesis promoted by endothelial cells prior to vascular function. Science 294, 559–563.

Mochizuki, T., Tsuchiya, K., Yokoyama, T., 2002. Molecular cloning of a gene for inversion of embryo turning (inv) with cystic kidney. Nephrol. Dial. Transplant 17(Suppl. 9), 68–70.

Neumann, C.J., Grandel, H., Gaffield, W., Schulte-Merker, S., Nusslein-Volhard, C., 1999. Transient establishment of anteroposterior polarity in the zebrafish pectoral fin bud in the absence of sonic hedgehog activity. Development 126, 4817–4826.

Nishina, H., Vaz, C., Billia, P., Nghiem, M., Sasaki, T., De la Pompa, J.L., Furlonger, K., Paige, C., Hui, C., Fischer, K.D., Kishimoto, H., Iwatsubo, T., Katada, T., Woodgett, J.R., Penninger, J.M., 1999. Defective liver formation and liver cell apoptosis in mice lacking the stress signaling kinase SEK1/MKK4. Development 126, 505–516.

Nowicki, M.J., Poley, J.R., 1998. The hereditary hyperbilirubinaemias. Baillieres Clin. Gastroenterol. 12, 355–367.

Ober, E.A., Field, H.A., Stainier, D.Y., 2003. From endoderm formation to liver and pancreas development in zebrafish. Mech. Dev. 120, 5–18.

Pack, M., Solnica-Krezel, L., Malicki, J., Neuhauss, S.C., Schier, A.F., Stemple, D.L., Driever, W., Fishman, M.C., 1996. Mutations affecting development of zebrafish digestive organs. Development 123, 321–328.

Ransom, D.G., Haffter, P., Odenthal, J., Brownlie, A., Vogelsang, E., Kelsh, R.N., Brand, M., van Eeden, F.J., Furutani-Seiki, M., Granato, M., Hammerschmidt, M., Heisenberg, C.P., Jiang, Y.J., Kane, D.A., Mullins, M.C., Nusslein-Volhard, C., 1996. Characterization of zebrafish mutants with defects in embryonic hematopoiesis. Development 123, 311–319.

Rossi, J.M., Dunn, N.R., Hogan, B.L., Zaret, K.S., 2001. Distinct mesodermal signals, including BMPs from the septum transversum

mesenchyme, are required in combination for hepatogenesis from the endoderm. Genes Dev. 15, 1998–2009.

Sasado, T., Morinaga, C., Niwa, K., Shinomiya, A., Yasuoka, A., Suwa, H., et al., 2004. Mutations affecting early distribution of primordial germ cells in Medaka (*Oryzias latipes*) embryo. Mech. Dev. 121, 817–828.

Schier, A.F., Neuhauss, S.C., Harvey, M., Malicki, J., Solnica-Krezel, L., Stainier, D.Y., Zwartkruis, F., Abdelilah, S., Stemple, D.L., Rangini, Z., Yang, H., Driever, W., 1996. Mutations affecting the development of the embryonic zebrafish brain. Development 123, 165–178.

Schier, A.F., Neuhauss, S.C., Helde, K.A., Talbot, W.S., Driever, W., 1997. The one-eyed pinhead gene functions in mesoderm and endoderm formation in zebrafish and interacts with no tail. Development 124, 327–342.

Schilling, T.F., Concordet, J.P., Ingham, P.W., 1999. Regulation of left-right asymmetries in the zebrafish by Shh and BMP4. Dev. Biol. 210, 277–287.

Shafizadeh, E., Paw, B.H., Foott, H., Liao, E.C., Barut, B.A., Cope, J.J., Zon, L.I., Lin, S., 2002. Characterization of zebrafish merlot/chablis as non-mammalian vertebrate models for severe congenital anemia due to protein 4.1 deficiency. Development 129, 4359–4370.

Stainier, D.Y., Weinstein, B.M., Detrich, H.W. 3rd, Zon, L.I., Fishman, M.C., 1995. Cloche, an early acting zebrafish gene, is required by both the endothelial and hematopoietic lineages. Development 121, 3141–3150.

Tam, P.P., Kanai-Azuma, M., Kanai, Y., 2003. Early endoderm development in vertebrates: lineage differentiation and morphogenetic function. Curr. Opin. Genet. Dev. 13, 393–400.

Thisse, C., Zon, L., 2002. Organogenesis-heart and blood formation from the zebrafish point of view. Science 295, 457–462.

van Eeden, F.J., Granato, M., Schach, U., Brand, M., Furutani-Seiki, M., Haffter, P., Hammerschmidt, M., Heisenberg, C.P., Jiang, Y.J., Kane, D.A., Kelsh, R.N., Mullins, M.C., Odenthal, J., Warga, R.M., Nusslein-Volhard, C., 1996. Genetic analysis of fin formation in the zebrafish. Danio rerio. Development 123, 255–262.

Wada, T., Joza, N., Cheng, H.M., sasaki, T., Kozieradzki, I., Bachmaier, K., Katada, T., Schreiber, M., Wagner, E.F., Nishina, H., Penninger, J.M., 2004. MKK7 couples stress signaling to G2/M cell cycle progression and cellular senescence. Nat. Cell Biol. 6, 215–226.

Wallace, K.N., Pack, M., 2003. Unique and conserved aspects of gut development in zebrafish. Dev. Biol. 255, 12–29.

Warga, R.M., Stainier, D.Y., 2002. The guts of endoderm formation. Results Probl. Cell Differ. 40, 28–47.

Watanabe, T., Nakagawa, K., Ohata, S., Kitagawa, D., Nishitai, G., Seo, J., Tanemura, S., Shimizu, N., Kishimoto, H., Wada, T., Aoki, J., Arai, H., Iwatsubo, T., Mochita, M., Satake, M., Ito, Y., Matsuyama, T., Mak, T.W., Penninger, J.M., Nishina, H., Katada, T., 2002. SEK1/MKK4-mediated SAPK/JNK signaling participates in embryonic hepatoblast proliferation via a pathway different from NF-κB-induced anti-apoptosis. Dev. Biol. 250, 332–347.

Weistein, B., Schier, A., Abdelilar, S., Malicki, J., Solnica-Krezel, L., Stemple, D., Stainier, D.Y., Zwartkruis, F., Driever, W., Fishman, M., 1996. Hematopoietic mutations in the zebrafish. Development 123, 303–309.

Zaret, K.S., 2001. Hepatocyte differentiation: from the endoderm and beyond. Curr. Opin. Genet. Dev. 11, 568–574.

Zaret, K.S., 2002. Regulatory phases of early liver development: paradigms of organogenesis. Nat. Rev. Genet. 3, 499–512.

Zhang, J., Talbot, W.S., Schier, A.F., 1998. Positional cloning identifies zebrafish one-eyed pinhead as a permissive EGF-related ligand required during gastrulation. Cell 92, 241–251.

Glossary

hiohgi: a traditional Japanese hand fan for court functions;
kakurembo: a game of hide-and-seek;
kamifusen: a balloon made of paper;
origami: art of folding paper;
kendama: Japanese toy with a wooden cup and a ball on a thread, where one tries to catch the ball in the cup;
hanetsuki: traditional Japanese badminton using colored wooden racquets and a shuttlecock;
dendendaiko: a Japanse drum for children that makes a sound by turning it upside down;
akane, suou: traditional Japanese term for red;
ominaeshi: a traditional Japanese term for white;
uguisucha, ukon: traditional Japanese dark yellow color;
aonibi: dark green;
fukuwarai: Japanese jigsaw-puzzle to make with face blindfolded;
sakura: cherry blossom;
akebono: rising sun;
akatsuki,
mochizuki: full moon;
hirame: flounder

ELSEVIER

Available online at www.sciencedirect.com
SCIENCE DIRECT

Toxicology Letters 152 (2004) 175–181

Toxicology Letters

www.elsevier.com/locate/toxlet

Requirement of MKK4 and MKK7 for $CdCl_2$- or $HgCl_2$-induced activation of c-Jun NH_2-terminal kinase in mouse embryonic stem cells

Masato Matsuoka [a,b,*], Hideki Igisu [b], Kentaro Nakagawa [c], Toshiaki Katada [c], Hiroshi Nishina [c]

[a] *Department of Hygiene and Public Health (1), School of Medicine, Tokyo Women's Medical University, 8-1 Kawada-cho, Shinjuku-ku, Tokyo 162-8666, Japan*

[b] *Department of Environmental Toxicology, Institute of Industrial Ecological Sciences, University of Occupational and Environmental Health, 1-1 Iseigaoka, Yahatanishi-ku, Kitakyushu 807-8555, Japan*

[c] *Department of Physiological Chemistry, Graduate School of Pharmaceutical Sciences, University of Tokyo, 7-3-1 Hongo, Bunkyo-ku, Tokyo 113-0033, Japan*

Received 10 March 2004; received in revised form 27 April 2004; accepted 28 April 2004

Available online 15 June 2004

Abstract

c-Jun NH_2-terminal kinase (JNK), also known as stress-activated protein kinase (SAPK), is activated primarily by inflammatory cytokines and environmental stresses including toxic metal exposure. To reveal the upstream kinase responsible for JNK activation by toxic metals, the phosphorylation status and the activity of JNK were examined in mouse embryonic stem (ES) cells lacking MKK4 or MKK7 following exposure to $CdCl_2$ or $HgCl_2$. Treatment with $CdCl_2$ or $HgCl_2$ induced the phosphorylation of JNK in a dose- and time-dependent manner in wild-type ES cells. In both $mkk4^{-/-}$ and $mkk7^{-/-}$ ES cells, $CdCl_2$- or $HgCl_2$-induced phosphorylation and activation of JNK were suppressed significantly. However, in $mkk7^{-/-}$ ES cells treated with $CdCl_2$ and $HgCl_2$, JNK activation was not abolished (suppressed by 56% and 78%, respectively). These findings suggest that the full activation of JNK by toxic metal exposure requires both MKK4 and MKK7, and these upstream kinases might contribute differentially in JNK activation between mouse ES cells exposed to $CdCl_2$ and $HgCl_2$.
© 2004 Elsevier Ireland Ltd. All rights reserved.

Keywords: c-Jun NH_2-terminal kinase; MKK4; MKK7; $CdCl_2$; $HgCl_2$; ES cells

1. Introduction

Mitogen-activated protein kinases (MAPKs) are a family of Ser/Thr protein kinases that transmit signals into the nucleus, and have been shown to participate in a diverse array of cellular functions such as the control of gene expression, cell proliferation, differentiation, development, inflammatory response, and

Abbreviations: JNK, c-Jun NH_2-terminal kinase; SAPK, stress-activated protein kinase; ES, embryonic stem; MAPK, mitogen-activated protein kinase; ERK, extracellular signal-regulated protein kinase

* Corresponding author. Tel.: +81-3-3353-8111; fax: +81-3-5269-7419.
E-mail address: matsuoka@research.twmu.ac.jp (M. Matsuoka).

0378-4274/$ – see front matter © 2004 Elsevier Ireland Ltd. All rights reserved.
doi:10.1016/j.toxlet.2004.04.033

apoptosis in mammalian systems (Chang and Karin. 2001; Weston and Davis, 2002). c-Jun NH_2-terminal kinase (JNK), also known as stress-activated protein kinase (SAPK), represents one subgroup of MAPKs that is activated primarily by inflammatory cytokines and environmental stresses such as ultraviolet radiation, ionizing radiation, heat shock, osmotic shock, protein synthesis inhibitor, and chemical mutagens (Kyriakis and Avruch, 1996; Robinson and Cobb, 1997). In addition, we have found that environmentally contaminating toxic metals such as cadmium (Matsuoka and Igisu, 1998), inorganic mercury (Matsuoka et al., 2000), and tributyltin (Yu et al., 2000) activate JNK pathway. However, functions and molecular mechanisms of toxic metal-induced JNK activation have not yet been known.

For the activation, JNK requires the dual phosphorylation of Thr and Tyr residues located in a Thr-Pro-Tyr motif between kinase subdomains VII and VIII (Cobb and Goldsmith, 1995). This phosphorylation is catalyzed by the dual specific kinases MKK4 (also known as SEK1 or MEK4) and MKK7 (SEK2), while MKK4 has a preference for the Tyr residue and MKK7 for the Thr residue (Weston and Davis, 2002). In vitro, JNK is activated synergistically by these two upstream kinases (Lawler et al., 1998). With respect to cadmium, it has been reported that JNK activation was suppressed partially by expression of dominant negative mutant of MKK7, but not that of MKK4 in human non-small-cell lung carcinoma cells (Chuang and Yang, 2001; Chuang et al., 2000) and rat mesangial cells (Ding and Templeton, 2000). These findings suggest that cadmium might activate JNK through MKK7, but not MKK4 in vivo. On the other hand, the activation of JNK by ultraviolet, heat shock, sorbitol-induced osmolarity change, or the protein synthesis inhibitor anisomycin was markedly attenuated in mouse embryonic stem (ES) cells targeting either the *mkk4* or the *mkk7* gene (Kishimoto et al., 2003), indicating that both MKK4 and MKK7 are required for the activation of JNK by these stimuli in mouse ES cells. To clarify whether signaling pathway leading to JNK activation by toxic metals is distinct from the case of other cellular stresses, the phosphorylation status and the activity of JNK were examined in *mkk4*$^{-/-}$ and *mkk7*$^{-/-}$ ES cells following exposure to $CdCl_2$ or $HgCl_2$. The application of these ES cells lacking either MKK4 or MKK7 would be more beneficial than other cells expressed with dominant negative form of them.

2. Materials and methods

2.1. Cell culture and treatments

The murine ES cell line E14K (wild-type), *mkk4*$^{-/-}$ mutant cell line made by the *mkk4* gene targeting (Nishina et al., 1997), and *mkk7*$^{-/-}$ mutant cell line made by the *mkk7* gene targeting (Kishimoto et al., 2003) were maintained in Dulbecco's modified Eagle's medium supplemented with 15% fetal calf serum (GIBCO, Invitrogen Corp., Carlsband, CA, USA) and leukemia inhibitory factor as described previously (Kishimoto et al., 2003). Wild-type, *mkk4*$^{-/-}$ and *mkk7*$^{-/-}$ ES cells (passage number 10–15) were plated at 5×10^5 cells per well (for Western immunoblotting) or 1.6×10^6 cells per well (for JNK activity assay) in six-well culture plates coated with 1% gelatin, and cultured for overnight. Then, medium was changed to serum-free medium containing $CdCl_2$ (Sigma Chemical Co., St. Louis, MO, USA) or $HgCl_2$ (Nacalai Tesque, Osaka, Japan). Untreated control cells were incubated with serum-free medium, and were treated identically to cells incubated with $CdCl_2$ or $HgCl_2$. Initially, dose (1 μM, 5 μM, 10 μM, 20 μM, or 40 μM) and time (5 min, 15 min, 30 min, 45 min, or 60 min) of $CdCl_2$ or $HgCl_2$ exposure for the sufficient induction of JNK phosphorylation were determined in wild-type ES cells. Based on these experiments, each ES cell line was incubated with 20 μM of $CdCl_2$ or $HgCl_2$ for 1 h. All experiments were repeated three (for Western immunoblotting) or four times (for JNK activity assay). Data were all obtained from two independently derived ES cell clones with comparable results.

2.2. Western immunoblotting

After the incubation with $CdCl_2$ or $HgCl_2$, ES cells were washed with phosphate-buffered saline, and lysed with sodium dodecyl sulfate (SDS)-polyacrylamide gel Laemmli sample buffer. Cell lysates were collected, sonicated, and boiled for 5 min. Twenty micrograms of protein was subjected to SDS-polyacrylamide gel electrophoresis on a 10%

polyacrylamide gel and transferred to a nitrocellulose membrane (Hybond-ECL, Amersham Pharmacia Biotech, Buckinghamshire, England). The membrane was blocked with 5% non-fat milk or bovine serum albumin in Tris-buffered saline containing 0.1% Tween 20 for 1 h at room temperature. The membrane was incubated overnight at 4 °C with the primary antibody diluted 1:1000. The antibodies used were phospho-SAPK/JNK (Thr^{183}/Tyr^{185}) antibody, phosphorylation state-independent SAPK/JNK antibody, phospho-p38 MAPK (Thr^{180}/Tyr^{182}) antibody, phosphorylation state-independent p38 MAPK antibody, phospho-p44/42 MAPK (Thr^{202}/Tyr^{204}) antibody, phosphorylation state-independent p44/42 MAPK antibody, phospho-specific c-Jun (Ser^{63}) antibody (Cell Signaling Technology, Inc., Beverly, MA, USA), anti-ACTIVE JNK antibody (Promega Corporation, Madison, IL, USA), MEK-4 (C-20) antibody (Santa Cruz Biotechnology Inc., Santa Cruz, CA, USA), and rat monoclonal antibody against MKK7 (KN-004) prepared by Kishimoto et al. (2003). Protein was detected with a Phototope-HRP Western blot detection kit (Cell Signaling Technology). For the detection of MKK7 protein, a SuperSignal West Femto Maximum Sensitivity Substrate (Pierce Chemical Co., Rockford, IL, USA) was used. After the immunodetection, some blots were incubated with a Restore Western Blot Stripping Buffer (Pierce) for 30 min at room temperature, and reprobed with each phosphorylation state-independent MAPK antibody. The bands on the developed films were quantified with NIH Image Version 1.63.

2.3. JNK activity assay

The in vitro activity of JNK was measured using a SAPK/JNK assay kit (Cell Signaling Technology) according to the instruction from the manufacturer. Briefly, cell lysates were incubated with GST-c-Jun (1–89) fusion protein overnight, and the precipitated JNK was subjected to in vitro kinase assay using GST-c-Jun (1–89) as substrate. Phosphorylation of GST-c-Jun on Ser^{63} was analyzed with immunoblotting using phospho-c-Jun antibody. The bands on the developed films were quantified with NIH Image Version 1.63.

2.4. Statistical analysis

Results were expressed as mean ± S.D. The statistical significance was determined by one-way analysis of variance followed by the Dunnett multiple comparison test. $P < 0.05$ was considered as statistically significant.

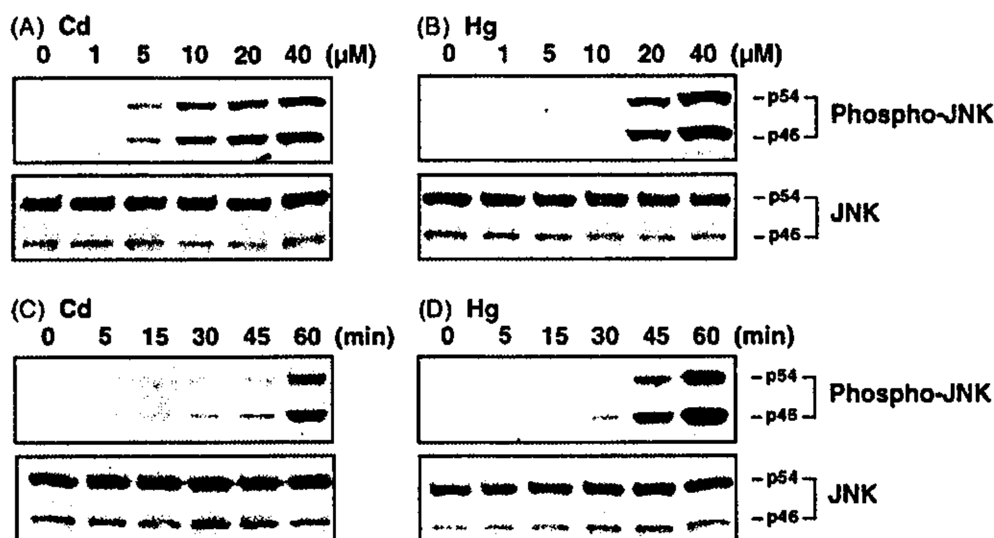

Fig. 1. Dose effects (A, B) and time course (C, D) of $CdCl_2$- or $HgCl_2$-induced accumulation of phosphorylated JNK in wild-type ES cells. Wild-type ES cells were incubated with 0 μM, 1 μM, 5 μM, 10 μM, 20 μM, or 40 μM $CdCl_2$ (A) or $HgCl_2$ (B) for 1 h. In the time course study, cells were incubated with 20 μM $CdCl_2$ (C) or $HgCl_2$ (D) for 5–60 min. The untreated control is 0 min. Cell lysates were subjected to immunoblotting using anti-phospho-JNK and anti-JNK antibodies. Results shown are representative of three independent experiments.

3. Results

3.1. $CdCl_2$- or $HgCl_2$-induced accumulation of phosphorylated JNK in wild-type ES cells

When wild-type ES cells were incubated with 5 μM of $CdCl_2$ or 20 μM of $HgCl_2$ for 1 h, phosphorylation of JNK (p46 and p54) was found, and the levels of phosphorylated form of JNK increased in a concentration-dependent manner (Fig. 1A and B). In contrast, the levels of total (phosphorylation state-independent) JNK were not changed by incubation with any concentration of $CdCl_2$ or $HgCl_2$. In the time course study, the levels of phosphorylated JNK increased after 30 min or 45 min in response to 20 μM $CdCl_2$ or $HgCl_2$ exposure, whereas total JNK levels were not changed (Fig. 1C and D). Thereafter, ES cells were exposed to $CdCl_2$ or $HgCl_2$ for 1 h at a concentration of 20 μM.

3.2. Suppression of $CdCl_2$- or $HgCl_2$-induced JNK activation in $mkk4^{-/-}$ and $mkk7^{-/-}$ ES cells

As shown in Fig. 2, MKK4 and MKK7 proteins were not detected in $mkk4^{-/-}$ and $mkk7^{-/-}$ ES cells, respectively. Neither MKK4 expression in wild-type and $mkk7^{-/-}$ ES cells nor MKK7 expression in wild-type and $mkk4^{-/-}$ ES cells was affected by the treatment with $CdCl_2$ or $HgCl_2$. In $mkk4^{-/-}$ ES cells, $CdCl_2$- or $HgCl_2$-induced phosphorylation of JNK was abolished almost completely without changing JNK levels (Fig. 3A, lanes 5 and 6). While toxic metal-induced JNK phosphorylation in $mkk7^{-/-}$ ES cells was also reduced significantly, JNK phosphorylation in $mkk7^{-/-}$ ES cells treated with $CdCl_2$ and $HgCl_2$ was 55% and 33% of that in wild-type ES cells treated, respectively (Fig. 3A, lanes 8 and 9). These findings were reproducible with two different anti-phospho-JNK antibodies used in the present study. In contrast to JNK, substantial phosphorylation of other members of MAPK family, p38 and extracellular signal-regulated protein kinase (ERK2/p42 and ERK1/p44), were observed in both, $mkk4^{-/-}$ and $mkk7^{-/-}$ ES cells treated with $CdCl_2$ or $HgCl_2$ (Fig. 3B and C, lanes 5, 6, 8 and 9).

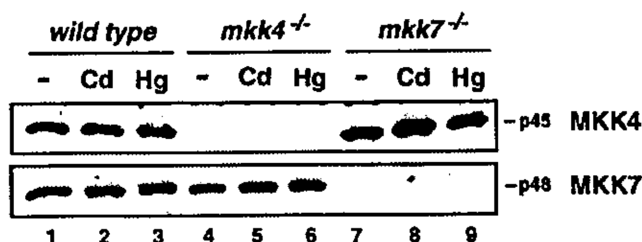

Fig. 2. Effects of $CdCl_2$ or $HgCl_2$ treatment on the levels of MKK4 and MKK7 in wild-type, $mkk4^{-/-}$ and $mkk7^{-/-}$ ES cells. Wild-type, $mkk4^{-/-}$ and $mkk7^{-/-}$ ES cells were incubated with serum-free medium (lanes 1, 4, and 7), 20 μM $CdCl_2$ (lanes 2, 5, and 8) or 20 μM $HgCl_2$ (lanes 3, 6, and 9) for 1 h, and cell lysates were subjected to immunoblotting using anti-MKK4 and anti-MKK7 antibodies. Results shown are representative immunoblot of three independent experiments.

The in vitro activity of JNK assayed using GST-c-Jun as substrate was also examined. Treatment with $CdCl_2$ or $HgCl_2$ induced the marked elevation of JNK activity in wild-type ES cells (Fig. 4, lanes 2 and 3). Consistent with the reduction of phosphorylated JNK levels (Fig. 3A), $CdCl_2$- or $HgCl_2$-induced JNK activation was suppressed in both $mkk4^{-/-}$ and $mkk7^{-/-}$ ES cells. JNK activity in $mkk4^{-/-}$ ES cells treated with $CdCl_2$ and $HgCl_2$ was 12% and 11% of that in wild-type ES cells treated, respectively (Fig. 4, lanes 5 and 6). JNK activity in $mkk7^{-/-}$ ES cells treated with $CdCl_2$ and $HgCl_2$ was 44% and 22% of that in wild-type ES cells treated, respectively (Fig. 4, lanes 8 and 9). Determination of JNK activity based on $[\gamma - ^{32}P]$ incorporation into GST-c-Jun also showed the significant reduction of $CdCl_2$-induced JNK activation in both, $mkk4^{-/-}$ and $mkk7^{-/-}$ ES cells (Nakagawa et al., unpublished data).

4. Discussion

The present study showed that treatment with $CdCl_2$ or $HgCl_2$ induced the accumulation of phosphorylated form of JNK in a dose- and time-dependent manner in wild-type ES cells as has been observed in the various cell types (Matsuoka and Igisu, 2002). In both, $mkk4^{-/-}$ and $mkk7^{-/-}$ ES cells which lack an upstream JNK activator, $CdCl_2$- or $HgCl_2$-induced phosphorylation and activation of JNK were suppressed dramatically. However, in $mkk7^{-/-}$ ES cells treated with $CdCl_2$ and $HgCl_2$, JNK activation was not abolished (suppressed by 56% and 78%, respectively). On the other hand, significant phosphorylation of other members of MAPK, p38 and ERK, was retained in

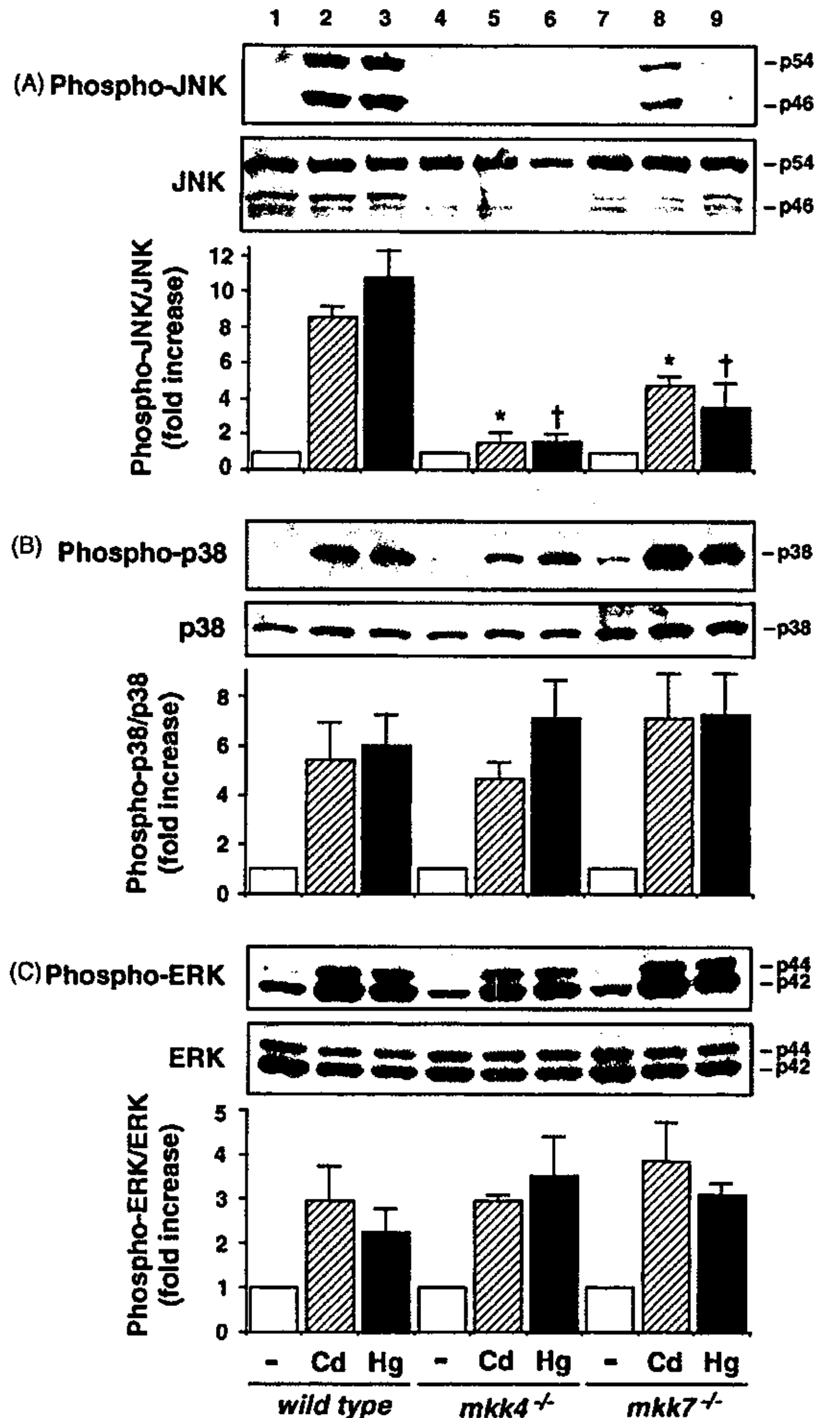

Fig. 3. Effects of $CdCl_2$ or $HgCl_2$ treatment on the levels of phosphorylated JNK (A), phosphorylated p38 (B), and phosphorylated ERK (C). Wild-type, *mkk4*$^{-/-}$ and *mkk7*$^{-/-}$ ES cells were incubated with serum-free medium (lanes 1, 4, and 7), 20 μM $CdCl_2$ (lanes 2, 5, and 8) or 20 μM $HgCl_2$ (lanes 3, 6, and 9) for 1 h, and cell lysates were subjected to immunoblotting using anti-phospho-JNK and anti-JNK antibodies (A), anti-phospho-p38 and anti-p38 antibodies (B), and anti-phospho-ERK and anti-ERK antibodies (C). Results shown are representative immunoblot and densitometric analysis of phosphorylated JNK, p38 and ERK. Each value was expressed as the ratio of phosphorylated MAPK level to the corresponding total MAPK level, and the value of control (without metal treatments) was set to one. Each column and bar represent the mean ± S.D. of three independent experiments. * $P < 0.01$ compared to wild-type ES cells treated with $CdCl_2$, † $P < 0.01$ compared to wild-type ES cells treated with $HgCl_2$.

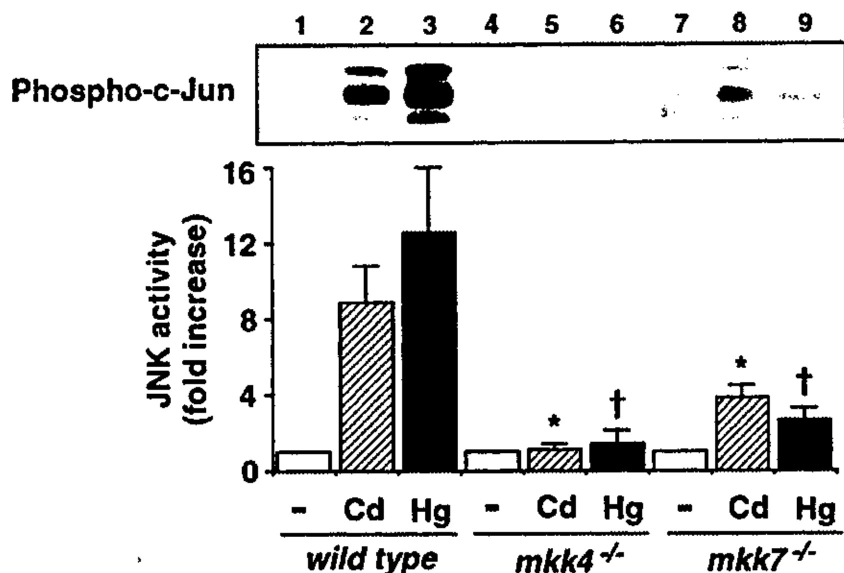

Fig. 4. Effects of $CdCl_2$ or $HgCl_2$ treatment on the activity of JNK in wild-type, *mkk4*$^{-/-}$ and *mkk7*$^{-/-}$ ES cells. Wild-type, *mkk4*$^{-/-}$ and *mkk7*$^{-/-}$ ES cells were incubated with serum-free medium (lanes 1, 4, and 7), 20 μM $CdCl_2$ (lanes 2, 5, and 8) or 20 μM $HgCl_2$ (lanes 3, 6, and 9) for 1 h, and cell lysates were used for in vitro kinase reaction with GST-c-Jun (1–89) as substrate. Phosphorylation of GST-c-Jun was analyzed with immunoblotting using anti-phospho-c-Jun antibody. Results shown are representative immunoblot and densitometric analysis of phosphorylated c-Jun. Each value was expressed as the fold increase with respect to the corresponding control (without metal treatments). Each column and bar represent the mean ± S.D. of four independent experiments. $^{*}P < 0.01$ compared to wild-type ES cells treated with $CdCl_2$, $^{\dagger}P < 0.01$ compared to wild-type ES cells treated with $HgCl_2$.

these mutated cell lines. These findings suggest that the full activation of JNK by toxic metal exposure requires both MKK4 and MKK7, and these upstream kinases might contribute differentially in JNK activation between ES cells exposed to $CdCl_2$ and $HgCl_2$. $CdCl_2$-induced JNK activation seems to depend on MKK4 more extensively than MKK7.

In contrast, previous studies using cells transfected with dominant-negative form of MKK4 or MKK7 showed that cadmium might activate JNK through MKK7, but not MKK4. Transfection with MKK4 mutant elevated $CdCl_2$ (80 μM, 3 h exposure) -induced JNK activation 1.9-fold in human non-small-cell lung carcinoma cells, while expression of MKK7 mutant reduced JNK activity by 35% (Chuang and Yang, 2001). However, expression of MKK7 mutant failed to suppress JNK activity in the same cells treated with a higher concentration of $CdCl_2$ (130 μM) (Chuang et al., 2000). In rat mesangial cells, $CdCl_2$ (10 μM, 8 h exposure) -induced JNK activation was suppressed by 53% when transfected with MKK7 mutant, but not changed by expression of MKK4 mutant (Ding and Templeton, 2000). On the other hand, it has been reported that treatment with $CdCl_2$ induced the phosphorylation of MKK4 in Rat-1 fibroblasts (Iordanov and Magun, 1999), and we also found the phosphorylation of MKK4 on Thr^{261} in wild-type ES cells following exposure to $CdCl_2$ or $HgCl_2$ (data not shown). Thus, MKK4 could be activated by upstream kinase (i.e., MAPK kinase kinase) in response to $CdCl_2$ or $HgCl_2$ exposure, and disruption of the *mkk4* gene abolished toxic metal-induced JNK activation almost completely in ES cells. While the precise functions of MKK4 and MKK7 in cells exposed to toxic metal are still not clear, these MAPK kinases might play a different role in JNK activation depending on the cell type and the experimental condition of exposure. With respect to mkk4$^{-/-}$ and *mkk7*$^{-/-}$ ES cells exposed to $CdCl_2$ or $HgCl_2$, the roles of splice variants and the effects of JNK (p46) expression remain to be examined.

In summary, as has been shown in various stress-induced JNK activation (Kishimoto et al., 2003; Wada et al., 2001), both MKK4 and MKK7 were required for the full activation of JNK in mouse ES cells exposed to $CdCl_2$ or $HgCl_2$. The *mkk4*$^{-/-}$ and *mkk7*$^{-/-}$ ES cells seem to be useful to analyze functions and signaling pathway of JNK activation induced by environmental stresses including toxic metals.

Acknowledgements

We thank Takeo Okuno for technical help. This work was supported in part by Grant-in-Aid for Scientific Research (KAKENHI: 14570313 and 14570315) from the Ministry of Education, Culture, Sports, Science and Technology (MEXT), Japan.

References

Chang, L., Karin, M., 2001. Mammalian MAP kinase signalling cascades. Nature 410, 37–40.

Chuang, S.-M., Yang, J.-L., 2001. Comparison of roles of three mitogen-activated protein kinases induced by chromium (VI) and cadmium in non-small-cell lung carcinoma cells. Mol. Cell. Biochem. 222, 85–95.

Chuang, S.-M., Wang, I.-C., Yang, J.-L., 2000. Roles of JNK, p38 and ERK mitogen-activated protein kinases in the growth inhibition and apoptosis induced by cadmium. Carcinogenesis 21, 1423–1432.

Cobb, M.H., Goldsmith, E.J., 1995. How MAP kinases are regulated. J. Biol. Chem. 270, 14843–14846.

Ding, W., Templeton, D.M., 2000. Stress-activated protein kinase-dependent induction of *c-fos* by Cd^{2+} is mediated by MKK7. Biochem. Biophys. Res. Commun. 273, 718–722.

Iordanov, M.S., Magun, B.E., 1999. Different mechanisms of c-Jun NH_2-terminal kinase-1 (JNK1) activation by ultraviolet-B radiation and by oxidative stressors. J. Biol. Chem. 274, 25801–25806.

Kishimoto, H., Nakagawa, K., Watanabe, T., Kitagawa, D., Momose, H., Seo, J., Nishitai, G., Shimizu, N., Ohata, S., Tanemura, S., Asaka, S., Goto, T., Fukushi, H., Yoshida, H., Suzuki, A., Sasaki, T., Wada, T., Penninger, J.M., Nishina, H., Katada, T., 2003. Different properties of SEK1 and MKK7 in dual phosphorylation of stress-induced activated protein kinase SAPK/JNK in embryonic stem cells. J. Biol. Chem. 278, 16595–16601.

Kyriakis, J.M., Avruch, J., 1996. Sounding the alarm: protein kinase cascades activated by stress and inflammation. J. Biol. Chem. 271, 24313–24316.

Lawler, S., Fleming, Y., Goedert, M., Cohen, P., 1998. Synergistic activation of SAPK1/JNK1 by two MAP kinase kinases in vitro. Curr. Biol. 8, 1387–1390.

Matsuoka, M., Igisu, H., 1998. Activation of c-Jun NH_2-terminal kinase (JNK/SAPK) in LLC-PK_1 cells by cadmium. Biochem. Biophys. Res. Commun. 251, 527–532.

Matsuoka, M., Igisu, H., 2002. Effects of heavy metals on mitogen-activated protein kinase pathways. Environ. Health Prev. Med. 6, 210–217.

Matsuoka, M., Wispriyono, B., Iryo, Y., Igisu, H., 2000. Mercury chloride activates c-Jun N-terminal kinase and induces *c-jun* expression in LLC-PK_1 cells. Toxicol. Sci. 53, 361–368.

Nishina, H., Fischer, K.D., Radvanyi, L., Shahinian, A., Hakem, R., Rubie, E.A., Bernstein, A., Mak, T.W., Woodgett, J.R., Penninger, J.M., 1997. Stress-signalling kinase Sek1 protects thymocytes from apoptosis mediated by CD95 and CD3. Nature 385, 350–353.

Robinson, M.J., Cobb, M.H., 1997. Mitogen-activated protein kinase pathways. Curr. Opin. Cell Biol. 9, 180–186.

Wada, T., Nakagawa, K., Watanabe, T., Nishitai, G., Seo, J., Kishimoto, H., Kitagawa, D., Sasaki, T., Penninger, J.M., Nishina, H., Katada, T., 2001. Impaired synergistic activation of stress-activated protein kinase SAPK/JNK in mouse embryonic stem cells lacking SEK1/MKK4: different contribution of SEK2/MKK7 isoforms to the synergistic activation. J. Biol. Chem. 276, 30892–30897.

Weston, C.R., Davis, R.J., 2002. The JNK signal transduction pathway. Curr. Opin. Genet. Dev. 12, 14–21.

Yu, Z., Matsuoka, M., Wispriyono, B., Iryo, Y., Igisu, H., 2000. Activation of mitogen-activated protein kinases by tributyltin in CCRF-CEM cells: role of intracellular Ca^{2+}. Toxicol. Appl. Pharmacol. 168, 200–207.